HHS Public Access

Author manuscript

J Bone Miner Res. Author manuscript; available in PMC 2020 April 01.

Published in final edited form as:

J Bone Miner Res. 2019 April ; 34(4): 681–698. doi:10.1002/jbmr.3635.

Probiotic *Lactobacillus reuteri* prevents post-antibiotic bone loss by reducing intestinal dysbiosis and preventing barrier disruption

Jonathan D Schepper[1], **Fraser Collins**[1], **Naiomy Deliz Rios-Arce**[1,2], **Sandi Raehtz**[1], **Laura Schaefer**[3], **Joseph D. Gardinier**[4], **Robert Britton**[3], **Narayanan Parameswaran**[1,5], and **Laura R McCabe**[1,5]

[1]Department of Physiology, Michigan State University, East Lansing, Michigan

[2]Comparative Medicine and Integrative Biology Program, Michigan State University, East Lansing, Michigan

[3]Department of Molecular Virology and Microbiology, Baylor College of Medicine

[4]Henry Ford Health System-Bone and Joint Center

[5]equal contribution and co-senior authors

Abstract

Antibiotic treatment, commonly prescribed for bacterial infections, depletes and subsequently causes long-term alterations in intestinal microbiota composition. Knowing the importance of the microbiome in the regulation of bone density, we investigated the effect of post-antibiotic treatment on gut and bone health. Intestinal microbiome repopulation at 4-weeks post-antibiotic treatment, resulted in an increase in the *Firmicutes:Bacteroidetes* ratio, increased intestinal permeability and notably reduced femoral trabecular bone volume (~30 %, $p<0.01$). Treatment with a mucus supplement (MDY) prevented the post-antibiotic induced barrier break as well as bone loss, indicating a mechanistic link between increased intestinal permeability and bone loss. A link between the microbiome composition and bone density was demonstrated by supplementing the mice with probiotic bacteria. Specifically, *Lactobacillus reuteri,* but not *Lactobacillus rhamnosus* GG or non-pathogenic *Escherichia coli*, reduced the post-antibiotic elevation of the *Firmicutes:Bacteroidetes* ratio and prevented femoral and vertebral trabecular bone loss. Consistent with causing bone loss, post-antibiotic induced dysbiosis decreased osteoblast and increased osteoclast activities, changes that were prevented by both *Lactobacillus reuteri* and MDY. These data underscore the importance of microbial dysbiosis in the regulation of intestinal permeability and bone health as well as identify *Lactobacillus reuteri* and MDY as novel therapies for preventing these adverse effects.

***Corresponding authors*:** Laura R McCabe Michigan State University, Department of Physiology and Department of Radiology, Biomedical Physical Science Building, 567 Wilson Road, East Lansing, MI 48824, Phone: (517) 884-5152, mccabel@msu.edu Narayanan Parameswaran, Michigan State University, Department of Physiology, Biomedical Physical Science Building, 567 Wilson Road, East Lansing, MI 48824, Phone: (517) 884-5115, narap@msu.edu.

Keywords

Microbiota; intestinal permeability; dysbiosis; antibiotic; trabecular bone; osteoblast; osteoclast; ampicillin

Introduction

The discovery in 1928 of the first antibiotic, penicillin, is one of the most important medical advances in the history of human health. Since that time, new classes of antibiotics have been developed and used to treat human bacterial infections (1). For this reason, antibiotic use is widespread resulting in more than 260 million prescriptions issued in the US in 2011 (2). Although antibiotics can be lifesaving, they also deplete commensal flora causing long-term changes in intestinal microbiota composition. This can impact overall health (3–9) and increase the risk for developing diseases such as inflammatory bowel disease (IBD) (10,11), obesity (12–14) and diabetes (15).

The intestinal microbiota includes ~100 trillion bacteria as well as fungi and viruses. Research has focused predominantly on gut bacteria composition which is thought to comprise of ~1000 bacterial species and 28 different phyla (7,16). *Firmicutes* and *Bacteroidetes* are the predominant phylum in the human intestine (17). The environment, diet, drugs and disease can affect microbiota composition (18–20) and lead to dysbiosis, an altered microbial community that contributes to disease. Dysbiosis has been linked to increased intestinal permeability/leaky gut (10,21) and is thought to be a key contributor to the pathogenesis of several diseases including IBD, obesity and diabetes (11,14,15).

Previous studies support a role for the gut microbiota in the regulation of bone health. For example, intestinal infection with pathogenic bacteria induces bone loss in male mice (22). In contrast, treatment with beneficial bacteria (probiotics) enhances bone density in healthy male mice (23), ovariectomized female mice (24–26), inflamed intact female mice (27), and type 1 diabetic male mice (28). Although earlier studies in germ free mice suggested a negative role for normal microbiota in bone health (29), subsequent findings have been inconsistent (24,30,31). This may be due to several factors including differences in the composition of the microbiota used to conventionalize germ free mice. For example, the presence of segmented filamentous bacteria can influence immune responses and osteoarthritis (32,33). In addition, past germ free studies have used various mouse strains (C57BL/6, BALB/c and Swiss Webster (29–31,34,35) which can further contribute to disparate responses. Finally, another confounding factor is that germ free mice have significantly altered immune systems (29,34) which can affect intestinal and bone signaling and responses.

Antibiotic treated and post-treated mice serve as additional models for investigating the roles of a depleted microbiome and dysbiosis, respectively, on organ health (36–39). Only a few studies to date have examined the effect of antibiotic treatment on bone health and most focused on the impact of chronic treatment. The results have been inconsistent, likely due to different treatment lengths, differences in age at the initiation of treatment and possibly differences in starting microbiome composition (40–43). Acute oral antibiotics deplete the

intestinal microbiome and subsequently alter the microbiota composition long after cessation of treatment (44,45). Very few studies have investigated the effects of a repopulated microbiome following antibiotic treatment, and none have investigated the effects on bone health in skeletally mature mice. Based on previous studies demonstrating the beneficial and harmful effects of probiotic and pathogenic bacteria respectively on bone health (22,23,25,28), we hypothesized that dysbiosis following antibiotic treatment would cause bone loss. To test this, we treated skeletally mature mice with oral antibiotics for 2 weeks to deplete the microbiome and allowed the treated mice to naturally repopulate the gut microbiome for 4 weeks. Our results demonstrate that although microbiota depletion per se has no effect on bone health, post-antibiotic dysbiosis markedly decreased bone density. Furthermore, we present evidence that the dysbiosis-induced bone loss is preventable by treatment with *Lactobacillus reuteri* and by enhancement of intestinal barrier function. Our studies underscore a key role for dysbiosis, following antibiotic treatment, in the pathogenic regulation of the gut-bone axis.

Methods

Animals and Experimental Design

Eleven-week old male BALB/c mice were obtained from Jackson Laboratories (Bar Harbor, ME). Mice were allowed to acclimate to the animal facility for 1-week prior to start of experiment. To deplete the commensal microbiota (15,46), at 12-weeks of age mice were treated with broad-spectrum antibiotics; ampicillin 1.0 g/L (Sigma, St. Louis, MO) and neomycin 0.5 g/L (Sigma, St. Louis, MO)(15,46), which are poorly absorbed by the intestine (47–49). Fresh antibiotics were given weekly into sterile drinking water; activity of the antibiotic-water was confirmed by its prevention of bacterial growth on agar plates. After 2-weeks, antibiotic treatment was stopped and mice were treated for 4-weeks with sterile drinking water (Aquavive water; Innovive, Dan Diego, CA) alone or containing 3.3×10^8 cfu/ml of either *Lactobacillus reuteri* 6475 (LR), *Lactobacillus rhamnosus* (LGG), non-pathogenic *E. coli* (EC, ATCC O6:B1) or 1.25 % MDY (a high molecular weight polymer used as a mucus supplement)(50,51). In addition, to assure adequate intake of bacteria the mice were gavaged 3 times a week with 300 ul of either broth (used for bacterial cultures) or 1×10^9 cfu/ml of the corresponding bacteria (LR, LGG, or EC). Experiments were repeated at least twice and the control and post-ABX mouse conditions were used in 5 separate experiments and gave similar responses in all runs. Mice were maintained on sterilized Teklad 2019 chow (Madison, WI) ad libitum and a 12 hr light/dark cycle in specific pathogen free conditions and housed in groups of 4–5 per cage. All animal procedures were approved by Michigan State University Institutional Animal Care and use Committee and conformed to NIH guidelines.

Bacterial culture

LR and LGG were cultured under anaerobic conditions on a de Man, Rogosa, Sharpe media (MRS, Difco) plates, while EC was cultured on Luria broth plates (LB, Invitrogen). Plates were kept at 37°C for a maximum of 1 week. For gavaging, single bacterial colonies were cultured in 10 ml of their respective broths. After 16–18 hours at 37° C, mice were gavaged with 300μl of bacteria (1×10^9 cfu/ml). When adding the bacteria to the drinking water, the

10 ml overnight culture was centrifuged at 5,000 RCF, re-suspended and cultured in fresh MRS/LB and grown until log phase (0D600 =0.4). Bacteria were pelleted, re-suspended in 60 mls of sterile PBS, stored in 1 ml aliquots at −80°C. Samples are thawed and subsequently re-suspended in sterile drinking water at a final concentration of 3.3×10^8 cfu/ml. Drinking water is changed 3X/week.

RNA analysis

Tibias were cleaned of muscle and connective tissue, flash frozen in liquid nitrogen and stored at −80°C. Frozen tibias were crushed under liquid nitrogen conditions with a Bessman Tissue Pulverizer (Spectrum Laboratories, Rancho Dominguez, CA). RNA was isolated using TriReagent (Molecular Research Center, Cincinnati, OH) and checked for integrity by agarose-gel electrophoresis. cDNA was produced by reverse transcription using Superscript II reverse transcriptase kit and oligo dT primers (Invitrogen, Carlsbad, CA). Intestines were flushed of their contents with 1X PBS and RNA isolated from mid colon sections. Gene expression levels were amplified by real-time PCR with iQ SYBR Green supermix (BioRad, Hercules, CA) and specific gene primers. Hypoxanthine guanine phosphoribosyltransferase (HPRT) mRNA levels, which do not change between treatment groups, were used as a house-keeping gene. PCR was carried out to 40 cycles using the iCycler (Bio-Rad) and data evaluated using the iCycler software. The cycle protocol consisted of 15 seconds at 95°C, 30 seconds at 60°C and 30 seconds at 72°C. Negative controls included primers without cDNA. Bacterial primers (targeted to bacterial specific 16S RNA (52)) were as follows: *Eubacteria* (Forward, **5'**- ACTCCTACGGGAGGCAGCAG- **3'**, Reverse, **5'**- ATTACCGCGGCTGCTGG- **3'**). Primers for mouse genes were as follows: *HPRT* (Forward, **5'**- AAGCCTAAGATGAGCGCAAG- **3'**, Reverse, **5'**- TTACTAGGCAGATGGCCACA), Osteocalcin (Forward, **5'**- AAGCAGGAGGGCAATAAGGT- **3'**, Reverse, **5'**- TAGGCGGTCTTCAAGCCAT- **3'**), TNF-α (Forward, **5'**- AGGCTGCCCCGACTACGT- **3'**, Reverse, **5'**- GACTTTCTCCTGGTATGAGATAGCAA- **3'**) and IL-10 (Forward, **5'**- TTGGAATCCCGAATTAACG- **3'**, Reverse, **5'**- GGTCACAGTGAAATACTGCTC- **3'**).

μCT Bone Imaging

Femurs, tibias and vertebrae were scanned using a GE Explore Locus microcomputed tomography at a resolution of 20 μm obtained from 720 views. Each scan had control and antibiotic treated bones and was phantom calibrated to maintain consistency. A fixed threshold of 980 (determined based on automated and isosurface analyses) was used for all bones. The distal femur trabecular bone region was defined as beginning proximal (a distance of 1 % of the total bone length) to the growth plate and then extending 10 % of bone length toward the diaphysis and excluding the cortical bone. Trabecular bone was also analyzed within the lumbar (L3) vertebrae. Trabecular bone parameters including volume, thickness, spacing and number values were obtained using GE Healthcare MicroView software version 2.2. Cortical measurements were performed in a 2×2×2 mm cube centered midway down the length of the bone. All bone analysis was performed blinded to the mouse condition.

Femoral Static and Dynamic Measures

For histomorphometric measures of bone formation, mice were intraperitoneally injected at 7 and 2 days prior to harvest with 200μl of 10-mg/ml sterile calcein (Sigma, St. Louis, MO) dissolved in sterile saline. Femurs were embedded in paraffin blocks and sectioned in 5 micron sections, as previously described (53). Distal femur metaphyseal sections were viewed with a fluorescent Nikon Eclipse E800 microscope (Nikon Instruments Inc, Melville, NY) and five digital images per section were taken. The distance between the calcein lines (mineral apposition rate, MAR) and the length of the calcein lines (single + double labeled surfaces; mineralized surface, MS) along the total bone surface (BS) were measured to calculate the bone formation rate (BFR) using Image Pro-Plus 7.0 (Media Cybernetics, Rockville, MD). Additionally, slides were stained for tartrate-resistant acid phosphatase (TRAP) activity and counterstained with hematoxylin according to manufacturer's protocol (387A-1KT; Sigma-Aldrich). TRAP-positive osteoclast number (Oc.N/BS) and surface (Oc.S/BS) were quantitated and expressed relative to the total bone surface. Histomorphometric measures were made blinded to the mouse condition. Standard nomenclature for JBMR was used for all bone histomorphometry measures (54).

Serum Measurements

Sterile blood was collected at the time of harvest, allowed to clot at room temperature for 5 minutes and then centrifuged at 5000g for 10 minutes. Serum was removed, aliquoted and snap frozen and in liquid nitrogen, and stored at −80°C. Serum tartrate resistant acid phosphatase 5b (TRAP5b) and osteocalcin (OC) were measured using mouse TRAP (Immunodiagnostic Systems Inc., Fountain Hills, AZ) and OC assay kits (Biomedical Technologies Inc., Stoughton, MA), respectively, according to manufacturer's protocol.

Mechanical Testing

Before testing, the $I_{A/P}$ and c were determined at the site of fracturing by microCT imaging as described above. Mechanical properties of the mouse tibias were then determined under four-point bending using an EnduraTech ELF 3200 Series (Bose®, MA)(55). The base support span was 9mm with a load span of 3mm. The tibia was positioned in the loading device so the medial surface was in tension by placing the most distal portion of the tibia and fibula junction directly over the left-most support. Each tibia was loaded at 0.01 mm/s until failure, while the load and displacement were recorded. The force-deflection curve then used to calculate the structural-level properties, while tissue-level properties were estimated using the following beam-bending equations: Stress = $\sigma = f \cdot a \cdot c / 2 \cdot I_{A/P}$; Strain = $\varepsilon = 6 \cdot c \cdot d / a (3 \cdot L - 4 \cdot a)$. In each equation, f is the applied force, d is the resulting displacement, a is the distance between the inner spans (3mm), L is the distance of the outer spans (9mm), $I_{A/P}$ is the moment of inertia about the anterior/posterior axis, and c is the distance from the neutral axis to the medial surface under tension. The yield point was determined from the stress-strain relationship using a 20% offset method (56). Mechanical testing was done blinded to conditions.

In vivo Intestinal Permeability

For whole intestinal permeability, mice were gavaged with 300 mg/kg of 4kD fluorescein isothiocyanate dextran (FITC) in sterile PBS 4 hours prior to time of death. Sterile serum was collected via cardiac puncture. Serum fluorescence was analyzed using a Tecan Infinite M1000 fluorescent plate reader at an excitation/emission wavelength of 485/530 nm. The rate of 4kD FITC-dextran transfer into the serum was calculated and normalized to control mouse measures for each day of the experiment.

Ex Vivo Ussing Chamber Intestinal Permeability

Mice were harvested and segments of the mid-distal colon removed. Sections were mounted in Lucite chambers and placed in Ussing chambers (physiologic Instruments, San Diego, CA, USA) exposing mucosal and serosal surfaces to oxygenated (95 % O_2, 5 % CO_2) Krebs bicarbonate ringer buffer (Sigma, St, Louis, MO, USA). Buffer was maintained at 37°C by a heated water jacket and samples allowed to equilibrate for 20 minutes. For measurements of tissue flux, 4 kDa FITC-dextran (2.2 mg/ml final concentration) was added to the mucosal side of the chamber. 10 kDa rhodamine B isothiocyanate (RITC)-dextran (0.55mg/ml final concentration) was also added to the mucosal chamber to control for tissue integrity. Serosal chamber samples were taken at 0 and 60 minutes and fluorescence intensity determined (FITC excitation, 485 nm; emission, 530nm; RITC excitation, 595nm; emission, 615nm; Tecan). FITC-dextran/RITC dextran concentrations were determined using a standard curve and FITC-dextran flux calculated.

DNA preparation of fecal samples

Fecal samples were transferred to Mo Bio Ultra Clean Fecal DNA bead Tubes (MoBio) containing 360µl of buffer ATL (Qiagen) and homogenized for one minute in a BioSpec Mini-Beadbeater. 40µL Proteinase K (Qiagen) was added and samples were incubated for 30 minutes at 55°C, then homogenized again for one minute and incubated at 55°C for additional 30 minutes. DNA was extracted with Qiagen DNeasy Blood and Tissue kit.

DNA extraction from mouse fecal samples, 16S rRNA gene amplification, and sequencing

DNA for microbial sequence analysis was extracted from mouse fecal samples by bead-beating and modified extraction with Qiagen DNeasy Blood and Tissue kits as described previously (25,30). Bacterial 16S sequences spanning variable region V4 were amplified by PCR with primers F515/R806 with a dual indexing approach and sequenced by Illumina MiSeq described previously(57). 20µl PCR reactions were prepared in duplicate and contained 40ng DNA template, 1X Phusion High-Fidelity Buffer (New England Biolabs), 200 µMdNTPs (Promega or Invitrogen), 10 nM primers, 0.2 units of Phusion DNA Polymerase (New England Biolabs), and PCR grade. Reactions were performed in an Eppendorf Pro thermal cycler with an initial denaturation at 98 °C for 30 s, followed by 30 cycles of 10 s at 98 °C, 20 s at 51 °C, and 1 min at 72 °C. Replicates were pooled and purified with Agencourt AMPure XP magnetic beads (Beckman Coulter). DNA samples were quantified using the QuantIt High Sensitivity DNA assay kit (Invitrogen) and pooled at equilmolar ratios. The quality of the pooled sample was evaluated with the Bioanalyzer High Sensitivity DNA Kit (Agilent).

Microbial community analysis

Sequence data was processed using the MiSeq pipeline for mothur using software version 1.38.1 (58) as described previously(30). In brief, forward and reverse reads were aligned, sequences were quality trimmed and aligned to the Silva 16S rRNA gene reference database formatted for mother, and chimeric sequences were identified and removed using the mothur implementation of UCHIME. Sequences were classified according to the mothur-formatted Ribosomal Database Project (version 16, February 2016) using the Bayesian classifier in mothur, and those sequences classified as Eukarya, Archaea, chloroplast, mitochondria, or unknown were removed. The sequence data were then filtered to remove any sequences present only once in the data set. After building a distance matrix from the remaining sequences with the default parameters in mothur, sequences were clustered into operational taxonomic units (OTUs) with 97 similarity using the average-neighbor algorithm in mothur. 871 OTUs were identified across all samples with an average rarefaction depth of 54,791 reads per sample. Alpha and beta diversity analyses and visualization of microbiome communities were performed with R, utilizing the phyloseq package (59,60). The Bray-Curtis dissimilarity matrix was used to describe differences in microbial community structure. Analysis of similarity (ANOSIM) was performed in mothur.

Statistical analysis

All measurements are presented as the mean ± SE. Significant outliers were removed using the ROUT test (5 total outliers were found with 1 maximum outlier detected per treatment group). All outliers excluded from data analysis shown in red. Student's t-test and 1-way ANOVA with Tukey post-test were performed using GraphPad Prism software version 7 (GraphPad, San Diego, CA, USA). A p-value ≤ 0.05 was considered significant and <0.01 highly significant.

Results

Natural repopulation following antibiotic treatment causes dysbiosis in mice

To deplete the intestinal microbiota, we treated 12-week old male BALB/c mice with broad-spectrum antibiotics, ampicillin (1 g/L) and neomycin (0.5 g/L), for 2 weeks. Microbiota depletion in antibiotic treated (ABX) mice was confirmed by a significant decrease in fecal bacterial colonies observed on agar dishes 24 hours after plating ($p<0.0001$; Fig 1A) and decreased colonic bacterial 16S rRNA DNA levels ($p<0.001$; Fig 1A). ABX-treated mice were allowed to naturally repopulate their microbiota during the next 4 weeks after which the gut microbiome was analyzed to assess if communities had recovered to their initial composition (Fig 1B). Analysis of colonic 16S rRNA bacterial levels indicated that there were no differences in bacterial load between 4-week post-ABX mice and controls (Fig 1C). However, the composition of the repopulated microbiome in post-ABX-treated mice was different compared to control mice. Post-ABX mice displayed changes in major phyla, specifically *Firmicutes* levels were increased and *Bacteroidetes* levels were decreased (Fig 1D). Diversity metrics that utilize species richness and evenness (Bray-Curtis) also showed a statistically significant separation between the ABX and control groups ($R=0.392$ $p<0.002$; Fig 1E). These data indicate that post-ABX mice develop an altered, potentially dysbiotic gut microbiota.

Antibiotic-induced dysbiosis decreases trabecular bone density.

To understand the effects of post-ABX dysbiosis on bone health parameters, we assessed femur trabecular bone density (Fig 2A). While ABX-depletion of the microbiota (at 2 weeks of ABX treatment) had no significant effect on trabecular bone volume fraction ($p= 0.1466$, Fig 2B), the 4-week post-ABX mice displayed a significant decrease in bone volume (~30 %, Fig 2B). Analyses of femoral bone architecture indicated a decrease in trabecular thickness (Tb.Th; $p<0.01$) and increase in trabecular spacing (Tb.Sp; $p<0.05$) in the post-ABX compared to control mice (Fig 2C). No significant differences were seen in cortical bone parameters following microbiota depletion or dysbiosis (data not shown). These data indicate that while microbiome depletion per se does not affect bone volume, post-ABX dysbiosis was associated with bone loss.

Antibiotic-induced dysbiosis causes bone loss via gut barrier dysfunction

Previous studies have shown that increased intestinal permeability observed in diseases, such as IBD, is correlated with bone loss (50). Studies have also shown that ABX-induced dysbiosis can affect intestinal permeability (61,62). Thus we posited that ABX-induced dysbiosis decreases bone health through altering intestinal permeability (24). To test this directly, 2 week-ABX mice were given a high molecular weight polymer, MDY-1001 (MDY), or vehicle for 4 weeks after cessation of ABX treatment. MDY is a non-absorbed mucus supplement that has previously been used to protect the intestinal epithelial layer during radiation injury (63). *In vivo* intestinal permeability was determined by gavaging mice with 4-kDa FITC-dextran 4 hours prior to harvest and then measuring serum FITC levels at harvest. Examination of permeability at the 2-week ABX treatment time point demonstrated no significant effect on intestinal flux compared to controls (Figure 3A). As expected, ABX-induced dysbiosis significantly increased permeability as demonstrated by elevated serum FITC levels, and MDY treatment was effective in preventing the increase (Fig 3A). Consistent with *in vivo* permeability, *ex vivo* colon flux was not affected by the 2-week ABX treatment but was increased in the post-ABX-induced dysbiosis mice ($p<0.05$) and this trended to be reduced by MDY treatment ($p=0.07$, Fig 3B).

Next, we examined if MDY prevention of post-ABX-dysbiosis induced intestinal barrier dysfunction also prevents bone loss. As postulated, MDY treatment following ABX treatment prevented post-ABX induced femoral and vertebral bone loss ($p<0.05$, Fig 3C–D) as well as changes in femoral bone architecture (Fig 3E). Together, these data suggest that dysbiosis following ABX treatment causes intestinal barrier dysfunction leading to bone loss that is prevented by enhancing barrier function.

Post-ABX-induced bone loss is prevented by probiotic *Lactobacillus reuteri* administration.

To examine if treatment with probiotic bacteria could alter microbial repopulation and potentially overcome the effects of post-ABX dysbiosis, mice were supplemented with *L. reuteri* ATCC PTA 6475 (LR) bacteria immediately following antibiotic cessation. LR was selected based on previous studies demonstrating oral LR benefits bone health in different models of bone loss (23,27,28). LR or broth (vehicle) control were administered for 4-weeks continuously to post-ABX mice. In addition, another probiotic, *Lactobacillus rhamnosus* GG

(LGG) and a non-pathogenic bacterium *Escherichia coli* (EC, ATCC O6:B1) were included as treatment groups to determine response specificity. The relative abundance and composition of the intestinal microbiota was examined at the end of the study (Fig 4A). Analyses of diversity metrics, utilizing species richness and evenness (Bray-Curtis), showed significant separation between the control group (non-ABX) and all treated groups (Bray-Curtis R= 0.272, $p<0.001$, Fig 4B). However, no significant differences in diversity metrics were detected between post-ABX mice treated with broth versus any of the bacterial treatment groups (Fig 4B). In contrast, analysis of OTUs identified differences in major bacterial phyla between groups. Treatment with LR did not significantly alter the abundance of most phyla examined but was the only treatment to decrease the post-ABX increase in *Firmicutes:Bacteriodetes* ratio (by 63 %, Fig 4C). At the specific strain level, the post-ABX induced dysbiosis was characterized by an increase in *Firmicutes* and significantly decreased levels of *Bacteroidetes* ($p<0.0001$; Fig 4D). LGG and EC, on the other hand, significantly increased OTUs classified to the phylum *Verrucomicrobia* compared to control and post-ABX cohorts (by 20-fold and 3.9-fold, respectively; Fig 4D) and decreased levels of *Firmicutes* (2-fold) compared to post-ABX cohorts. Together, these results suggest that supplementation with different bacteria following ABX treatment can affect the repopulation of major phyla.

Knowing that bacterial supplementation altered the gut microbiota, we examined effects on bone density. As expected, post-ABX mice displayed a decrease in bone volume fraction (femur trabecular region) compared to untreated controls (Fig 5A, $p<0.001$). Interestingly, only LR treatment, not LGG or EC, prevented this bone loss (Fig 5B). Similarly, the post-ABX decrease in vertebral trabecular volume was prevented by LR supplementation ($p<0.01$; Fig 5B), but not by LGG or EC. Measures of femur trabecular microarchitecture were correspondingly modulated by post-ABX, changes only prevented by LR (Fig 5C). Pearson's correlation analyses demonstrated that femoral trabecular BV/TV negatively correlated with the *Firmicutes:Bacteroidetes* ratio ($r = -0.4256$, $p=0.0097$**; Fig 5D). Cortical bone parameters were not affected by bacterial supplementation (Table 2).

L. reuteri administration reverses ABX-dysbiosis-induced barrier leak

In Figure 3, we demonstrated that ABX-induced dysbiosis causes intestinal barrier disruption and identified that MDY treatment prevents barrier disruption and bone loss. To test if LR administration also prevents barrier disruption, we measured *in vivo* and *ex vivo* intestinal barrier function in control and post-ABX mice supplementation with broth, LR, LGG and EC. As shown in Figure 6A, ABX-dysbiosis-induced *in vivo* permeability was inhibited by LR treatment but not by LGG or EC (Fig 6A). Consistent with the *in vivo* intestinal flux data, post-ABX mice displayed a trend toward increased colon permeability, which was prevented with LR but not LGG or EC treatment ($p<0.05$, Fig 6B). Furthermore, all colon flux measures negatively correlated with femoral trabecular bone density ($r= -0.4235$, $p=0.0027$; Fig 5C). A compromised intestinal barrier in diseases such as IBD has been shown to skew gut inflammation towards a more pro-inflammatory state(64–66). Analyses of colon pro- and anti-inflammatory cytokine expression revealed that increased permeability in the post-ABX, dysbiotic cohort was accompanied by a trending increase in the TNF-α/IL-10 ratio (Fig 6D). Additionally, LR and MDY, which prevented barrier

dysfunction, reduced the TNF-α /IL-10 ratio to a level that was not significantly different from control mice (Fig 6D). Together, the data suggest that LR and MDY enhancement of intestinal barrier function prevents post-ABX gut inflammation and bone loss.

Analysis of Osteoblast/Osteoclast Bone Remodeling Markers

To determine whether the gut microbiota manipulations affect catabolic bone parameters, we measured markers of osteoclast activity. Osteoclast number, surface and serum levels of tartrate resistant alkaline phosphatase (TRAP) were increased in the post-ABX induced dysbiosis group (Fig 7A–C) and decreased by LR and MDY treatment (Fig 7A-C). LGG and EC treatment did not significantly affect osteoclast markers relative to post-ABX mice (Fig 7A–C).

Markers of bone formation were also affected in post-ABX and treated mice. Serum osteocalcin was decreased in the post-ABX cohort (Fig 8A; $p<0.05$); both LR and MDY treatments prevented the suppression (Fig 8A; $p<0.05$) while LGG and EC did not. Consistent with serum osteocalcin levels, mineral apposition rate (MAR) and bone formation rate (BFR) were decreased in the post-ABX mice, and LR and MDY (but not LGG or EC treatment) prevented the suppression (Fig 8B, C). These results suggest that gut microbiome repopulation and/or manipulations following ABX treatment affect both anabolic and catabolic processes in bone.

Analysis of Mechanical Strength Testing Properties

Gut microbiome alterations under chronic antibiotic treatment have been shown to impair whole-bone mechanical properties (43). Therefore, we investigated whether acute antibiotic-induced gut dysbiosis affected structural or tissue level properties. Comparisons across all treatment groups revealed no significant change in structural-level mechanical properties (Fig 9A, B). Analysis of tissue-level mechanical properties, which estimate material properties of bone, did not reveal differences between groups (Fig 9C, D). These results suggest that post-ABX microbial repopulation does not affect the overall strength and tissue properties of cortical bone in skeletally mature mice.

Discussion

Antibiotics save countless lives and can prevent the spread of pathogenic bacteria, however, a significant side-effect of antibiotics is that they also deplete the commensal microbiota (9,15,46). Increasing numbers of studies demonstrate a role for the intestinal bacteria, as well as its composition in the regulation bone health (11,23–25,27,30,67–69). In the present study we identify that repopulation of the microbiota following acute antibiotic treatment results in dysbiosis, increases intestinal permeability and has a detrimental effect on trabecular bone health. We further reveal that oral supplementation with the probiotic *L. reuteri* 6475 or direct inhibition of gut barrier leak significantly prevents trabecular bone loss and strengthens the role of the gut as a therapeutic target for bone health.

Antibiotics provide an effective way to deplete the microbiota (70–72) and are a means to understand 1) the requirement of the microbiota for bone health and 2) the consequence of subsequent microbial dysbiotic repopulation (37,44,45) on bone health. Our studies utilized

a 2-week treatment of ampicillin and neomycin to deplete the microbiome. Ampicillin and neomycin are poorly absorbed in the rodent intestine (47–49) and, when administered together, effectively kill a broad- spectrum of bacteria and deplete the intestinal microbiota (15,46). The depletion of bacteria, particularly the beneficial commensal bacteria, has been demonstrated to provide an environment conducive to dysbiotic bacterial repopulation (44,45,71). This doesn't occur under microbiota replete conditions, in part because commensal bacteria produce anti-bacterial factors that decrease invasion by new bacterial competitors (73). Interestingly, acute antibiotic use in humans has been demonstrated to cause long-term (in some cases 4-years) alterations to microbiota composition (ie: dysbiosis) (37,44,45,74). Thus, our model gave us the opportunity to study the consequences of dysbiosis on bone health.

In the current study, antibiotic treatment caused significant changes in microbial composition as evidenced by principle coordinate analyses (PCoA) and manifested in a substantial decrease in *Bacteroidetes,* a predominant phylum in healthy mice and humans (17,74–76). A decrease in *Bacteroidetes* abundance has been associated with pathologies such as IBD, IBS, and type 1 diabetes (10,17,68,69,77–79). While our treatment approaches did not shift the overall PCA fingerprint of the post-antibiotic treated mice, LR was able to reduce the *Firmicutes:Bacteroidetes* ratio and prevent bone loss, while LGG and EC did not affect the ratio or prevent bone loss. Interestingly, only mice treated with LGG or non-pathogenic EC displayed an increase in the phylum *Verrucomicrobia* that has recently been shown to be increased by pro-inflammatory high fat-high sugar diets (80). The responsiveness observed in *Bacteroidetes* level and the link of the *Firmicutes:Bacteroidetes* ratio to bone health is most likely due to the abundance of these phyla and therefore reduced variability in comparisons. Deeper analyses of specific strains are variable across repeated experiments performed at different times of the year and in different animal rooms. We hypothesize that it is not the specific microbiota composition that regulates bone health; rather it is the balance of "disease promoting" versus "health promoting" bacteria. Our data support this but further studies are needed to understand which specific groups of bacterial strains are "healthy" in this context.

How does post-ABX induced dysbiosis promote bone loss? Dysbiosis has been linked to increased intestinal permeability/leaky gut (10,21,62) which has been linked to bone loss in diseases such as IBD (11,22,24,69,81) Our analyses indicate that colon flux significantly negatively correlates with trabecular bone density. By directly inhibiting barrier permeability with MDY treatment, our studies demonstrate that dysbiosis-induced intestinal barrier break contributes to post-ABX bone loss. This is consistent with our previous report demonstrating that chickens infected with intestinal salmonella benefit from MDY treatment and do not lose trabecular bone compared to untreated birds (82). Because MDY is not absorbed, its benefits to bone health are a consequence of its effects on the intestine, thereby underscoring the importance of the gut-bone signaling axis as a therapeutic target for osteoporosis. Under conditions of decreased barrier function (increased permeability), bacteria and their factors can translocate across the intestinal epithelium and move throughout the blood stream (50,83). Factors that promote intestinal permeability such as detergents (ie: DSS) skews the gut towards a more pro-inflammatory state (81) that is often characterized by increased levels of pro-inflammatory factors such as TNF-α and/or decreased levels of anti-

inflammatory factors such as IL-10 (81,84). We used the colon TNF/IL-10 ratio as a marker of the balance between a pro-versus anti- inflammatory state. Post-ABX trended to increase TNF/IL-10 levels while MDY and LR trended to reduce the TNF/IL-10 ratio, suggesting a reduction in colon inflammation compared to post-ABX (dysbiotic) mice.

While previous studies have shown that probiotics can promote intestinal barrier function and reduce intestinal inflammation (24,62,85–88), in our studies only LR had this beneficial effect. Based on our current results, LR had the ability to alter the *Firmicutes:Bacteriodetes* ratio, strengthen intestinal barrier function and reduce intestinal inflammation while LGG did not. As expected, the non-pathogenic EC also did not influence these parameters. The ability of LR but not LGG to benefit gut and bone health was unexpected given that LGG has been elegantly shown to benefit bone health in ovariectomized mice and in male and female mice (24,89). It is possible that an effective response is dependent upon the specific dysbiosis/microbiota composition as well as the disease model, inflammatory status, sex, age and strain (24,27,28,90,91). LGG is known to differ from LR because of its requirement for epithelial cell interaction to mediate it effects(92). In addition, specific probiotic strains produce unique and varying combinations of biologically active metabolites and proteins that can benefit intestinal microbiome, inflammation and permeability (25,93,94).

Our studies demonstrate that post-ABX induced dysbiosis had a marked effect on trabecular bone parameters of both long bone and vertebral sites. This was observed in repeated experiments. On the other hand, cortical bone microarchitecture and strength were not affected. A response likely due to the length of the study which could be too short to see changes in the slow remodeling cortical bone, as we have seen in other mouse models (95). Additional analyses of bone anabolic and catabolic processes indicated that both are affected by dysbiosis. Specifically, dysbiosis significantly increased osteoclast markers and decreased osteoblast markers. Past studies examining dysbiosis and enhanced intestinal permeability-induced bone loss have reported a predominant suppression of anabolic markers and some enhancement of resorption markers (22,81,83,96). Our treatment groups also affected these parameters but only MDY and LR were able to significantly reverse the effect of post-ABX dysbiosis. This is consistent with previous reports showing that LR can increase mineral apposition, osteoblast number, serum osteocalcin and decrease osteoclast markers in other mouse models such as type 1 diabetes and estrogen deficiency (23,25,28).

Our studies show that the microbiota depletion seen at the 2-week time point of antibiotic treatment did not affect bone density measures. Our results are similar to some germ free mouse studies (24,30). Studies in germ free mice, however, are inconsistent in terms of bone growth and density (increase, decrease, no change)(24,25,29,31,97). Caveats to the germ-free model are that the mice have intestinal and immunological abnormalities (including fewer T cells and T cells skewed toward a Th2 phenotype)(21,29,98,99). While differences in mouse genetic strain, age, and sex can contribute to study variation, the differences in the microbiota composition used to conventionalize the germ-free mice could be a major factor in directing the final outcome. While both the germ-free and antibiotic models of microbiota depletion are useful, the antibiotic treatment model overcomes the issue of long-term absence of microbiota and its associated developmental abnormalities.

Previous chronic antibiotic treatment studies examining bone health predominantly focused on longer antibiotic treatment times and used young mice (1-month of age) that are undergoing bone growth rather than remodeling. For example, a study treating young C57BL/6J mice at weaning with penicillin, chlortetracycline, or vancomycin for 4-months found a decrease in bone mineral content in males but not females (100). Chronic antibiotic treatment of 4 week old C57BL/6J mice with ampicillin and neomycin for 16 weeks decreased femoral bone bending (43). Studies in female mice have been more variable. For instance, 1-month old female C57BL/6J mice treated for ~2 months with penicillin, vancomycin and a combination displayed an early increase in bone mineral content at 3 weeks, but by the end of the study (7 weeks) bone mineral content (BMC) did not differ from controls (40). Whereas, another study treating 2-month old female BALB/c mice with an antibiotic cocktail (ampicillin, vancomycin, metronidazole and neomycin) for 6 weeks showed a decrease in bone formation that was related to reduced IGF-1 (31) which is critical for postnatal bone growth (101,102). In our studies, we did not observe changes in serum IGF-1 levels (data not shown) or bone length, which suggests that IGF-1 does not play a role in microbiome-mediated bone remodeling in skeletally mature male mice. Together, these studies suggest that chronic antibiotic treatments can affect bone health in a sex-and age-dependent manner. Direct comparison between studies is complicated due to differences in treatment duration, sex, genetic strain, age and antibiotics used.

There has yet to be any clinical studies examining the effects of ABX and post-ABX treatment on bone health. However, there are clinical studies looking into antibiotics/probiotics and their effects on the gut microbiome. Past studies have shown that a common one-week antibiotic treatment regimen with clarithromycin and metronidazole resulted in marked compositional disturbances in the throat and the gut microbiota, which persisted for up to 4 years post treatment (44). In a recent study examining antibiotic perturbation in mice and humans (103), probiotics were shown to induce a different stool and mucosal microbiome repopulation that was maintained and therefore delayed recovery of the original pre-ABX microbiota. This study did not look at functional outcomes to systemic health following antibiotic induced alterations to the gut microbiota or probiotic treatment, so it is unclear which microbiota composition is most beneficial to the host.

In summary, it is now recognized that a healthy intestinal microbiota benefits overall host health. Our studies highlight the importance of microbiota composition and intestinal barrier function in regulating bone health and suggest that the period following antibiotic treatment could be important not only for intestinal health but also for bone health. Correcting dysbiosis, increasing barrier function, and decreasing intestinal inflammation can enhance gut and bone health. The mouse model serves as a straight forward way to study dysbiosis effects on bone and has implications for the treatment of bone loss linked to other conditions of dysbiosis such as inflammatory bowel disease, diabetes, menopause and poor dietary intake (high fat diets). Discovering the connection between the microbiome and bone health can speed identification of novel therapeutic targets for osteoporosis.

ACKNOWLEDGMENTS

The authors thank the Investigative Histology Laboratory in the Department of Physiology, Division of Human Pathology and the Biomedical Imaging Center at Michigan State University for their assistance with histology and imaging, respectively. The authors are also grateful to the staff of Campus Animal Resources for the excellent care of our animals. These studies were supported by funding from the National Institute of Health, grants RO1 DK101050 and RO1 AT007695. Authors' roles: Study design: JS, NP and LRM. Study conduct: JS. Data collection/analysis: JS, FC, NDA, SR, LS and JDD. Data interpretation: JS, LS, JDD, RB, NP and LRM. Drafting/Revising manuscript content: JS, FC, NDA, RB, NP and LRM. Approving final version of manuscript: All authors. Integrity of data analysis: JS, NP and LRM.

Funding: These studies were supported by funding from the National Institute of Health, grants RO1 DK101050 and AT007695.

References:

1. MacKenzie FM, Monnet DL, Gould IM, ARPAC Steering Group on behalf of the AS. Relationship between the number of different antibiotics used and the total use of antibiotics in European hospitals J Antimicrob Chemother [Internet]. Oxford University Press; 2006 9 [cited 2016 Oct 27];58(3):657–60. Available from: http://www.ncbi.nlm.nih.gov/pubmed/16854957
2. Hicks LA, Bartoces MG, Roberts RM, Suda KJ, Hunkler RJ, Taylor TH, et al. US outpatient antibiotic prescribing variation according to geography, patient population, and provider specialty in 2011 Clin Infect Dis [Internet]. Oxford University Press; 2015 5 1 [cited 2015 Sep 14];60(9):1308–16. Available from: http://cid.oxfordjournals.org/content/60/9/1308.full
3. Reikvam DH, Erofeev A, Sandvik A, Grcic V, Jahnsen FL, Gaustad P, et al. Depletion of Murine Intestinal Microbiota: Effects on Gut Mucosa and Epithelial Gene Expression Heimesaat M, editor. PLoS One [Internet]. Public Library of Science; 2011 3 21 [cited 2016 Sep 20];6(3):e17996 Available from: http://dx.plos.org/10.1371/journal.pone.0017996
4. Frank DN, St Amand AL, Feldman RA, Boedeker EC, Harpaz N, Pace NR. Molecular-phylogenetic characterization of microbial community imbalances in human inflammatory bowel diseases. Proc Natl Acad Sci U S A [Internet]. 2007 8 21 [cited 2016 Sep 10];104(34):13780–5. Available from: http://www.ncbi.nlm.nih.gov/pubmed/17699621
5. Blaser M Antibiotic overuse: Stop the killing of beneficial bacteria. Nature [Internet]. 2011 8 24 [cited 2018 Jan 7];476(7361):393–4. Available from: http://www.nature.com/doifinder/10.1038/476393a
6. Dethlefsen L, Relman DA. Incomplete recovery and individualized responses of the human distal gut microbiota to repeated antibiotic perturbation Proc Natl Acad Sci U S A [Internet]. National Academy of Sciences; 2011 3 15 [cited 2016 Sep 21];(Supplement 1):4554–61. Available from: http://www.ncbi.nlm.nih.gov/pubmed/20847294
7. Zhernakova A, Kurilshikov A, Bonder MJ, Tigchelaar EF, Schirmer M, Vatanen T, et al. Population-based metagenomics analysis reveals markers for gut microbiome composition and diversity. Science (80-) [Internet]. 2016 4 29 [cited 2018 Jan 7];352(6285):565–9. Available from: http://www.ncbi.nlm.nih.gov/pubmed/27126040
8. Ferrer M, Mendez-Garcia C, Rojo D, Barbas C, Moya A. Antibiotic use and microbiome function. Biochem Pharmacol [Internet]. 2017 6 15 [cited 2018 Jan 7];134:114–26. Available from: http://www.ncbi.nlm.nih.gov/pubmed/27641814
9. Perez-Cobas AE, Gosalbes MJ, Friedrichs A, Knecht H, Artacho A, Eismann K, et al. Gut microbiota disturbance during antibiotic therapy: a multi-omic approach. Gut [Internet]. 2013 11 [cited 2018 Jan 7];62(11):1591–601. Available from: http://www.ncbi.nlm.nih.gov/pubmed/23236009
10. Tamboli CP, Neut C, Desreumaux P, Colombel JF. Dysbiosis in inflammatory bowel disease Gut [Internet]. BMJ Publishing Group; 2004 1 1 [cited 2017 Oct 24];53(1):1–4. Available from: http://www.ncbi.nlm.nih.gov/pubmed/14684564
11. Loh G, Blaut M. Role of commensal gut bacteria in inflammatory bowel diseases. Gut Microbes [Internet]. Taylor & Francis; 2012 1 11 [cited 2016 Mar 22];3(6):544–55. Available from: http://www.tandfonline.com/doi/full/10.4161/gmic.22156

12. Fukuda S, Ohno H. Gut microbiome and metabolic diseases. Semin Immunopathol [Internet]. Springer Berlin Heidelberg; 2014 1 6 [cited 2016 Aug 30];36(1):103–14. Available from: http://www.ncbi.nlm.nih.gov/pubmed/24196453

13. Ley R, Turnbaugh P, Klein S, Gordon J. Human Gut microbes associated with obesity. Nature. 2006;(444):1022–3.

14. Kim K-A, Gu W, Lee I-A, Joh E-H, Kim D-H. High fat diet-induced gut microbiota exacerbates inflammation and obesity in mice via the TLR4 signaling pathway PLoS One [Internet]. Public Library of Science; 2012 1 16 [cited 2016 Jan 22];7(10):e47713 Available from: http://journals.plos.org/plosone/article?id=10.1371/journal.pone.0047713

15. Cani PD, Bibiloni R, Knauf C, Waget A, Neyrinck AM, Delzenne NM, et al. Changes in gut microbiota control metabolic endotoxemia-induced inflammation in high-fat diet-induced obesity and diabetes in mice. Diabetes [Internet]. 2008 6 1 [cited 2015 Mar 22];57(6):1470–81. Available from: http://diabetes.diabetesjournals.org/content/57/6Z1470.long

16. Abeles S, Jones M, Santiago-Rodriguez T, Ly M, Nelson K, Pride D. Microbial Diversity in individuals and their household contacts following typical antibiotic courses. Microbiome. 2016;

17. Mariat D, Firmesse O, Levenez F, Guimaraes V, Sokol H, Doré J, et al. The Firmicutes/Bacteroidetes ratio of the human microbiota changes with age BMC Microbiol [Internet]. BioMed Central; 2009 6 9 [cited 2017 Feb 20];9(1):123 Available from: http://bmcmicrobiol.biomedcentral.com/articles/10.1186/1471-2180-9-123

18. Spor A, Koren O, Ley R. Unravelling the effects of the environment and host genotype on the gut microbiome. Nat Rev Microbiol [Internet]. Nature Publishing Group; 2011 4 [cited 2016 Sep 1];9(4):279–90. Available from: http://www.nature.com/doifinder/10.1038/nrmicro2540

19. Kang SS, Jeraldo PR, Kurti A, Miller ME, Cook MD, Whitlock K, et al. Diet and exercise orthogonally alter the gut microbiome and reveal independent associations with anxiety and cognition. Mol Neurodegener [Internet]. 2014 9 13 [cited 2017 Feb 1];9(1):36 Available from: http://www.ncbi.nlm.nih.gov/pubmed/25217888

20. Huang EY, Inoue T, Leone VA, Dalal S, Touw K, Wang Y, et al. Using corticosteroids to reshape the gut microbiome: implications for inflammatory bowel diseases. Inflamm Bowel Dis [Internet]. NIH Public Access; 2015 5 [cited 2017 Feb 17];21(5):963–72. Available from: http://www.ncbi.nlm.nih.gov/pubmed/25738379

21. Tremaroli V, Backhed F. Functional interactions between the gut microbiota and host metabolism. Nat [Internet]. 2012 [cited 2017 Sep 13];489:242–9. Available from: http://pol.gu.se/digitalAssets/1380/1380853_tremaroli_b--ckhed_nature_2012.pdf

22. Irwin R, Lee T, Young VB, Parameswaran N, McCabe LR. Colitis induced bone loss is gender dependent and associated with increased inflammation. Inflamm Bowel Dis. NIH Public Access; 2013;19(8):1586.

23. McCabe LR, Irwin R, Schaefer L, Britton RA. Probiotic use decreases intestinal inflammation and increases bone density in healthy male but not female mice. J Cell Physiol [Internet]. 2013 8 [cited 2015 Jun 25];228(8):1793–8. Available from: http://www.ncbi.nlm.nih.gov/pubmed/23389860

24. Li J-YJJ-YJ, Chassaing B, Tyagi AMA, Vaccaro C, Luo T, Adams J, et al. Sex steroid deficiency-associated bone loss is microbiota dependent and prevented by probiotics. J Clin Invest [Internet]. American Society for Clinical Investigation; 2016 4 25 [cited 2016 Aug 30];126(6):2049–63. Available from: https://www.jci.org/articles/view/86062

25. Britton RA, Irwin R, Quach D, Schaefer L, Zhang J, Lee T, et al. Probiotic L. reuteri Treatment Prevents Bone Loss in a Menopausal Ovariectomized Mouse Model. J Cell Physiol [Internet]. NIH Public Access; 2014 11 [cited 2017 Jan 16];229(11):1822–30. Available from: http://doi.wiley.com/10.1002/jcp.24636

26. Ohlsson C, Engdahl C, Fäk F, Andersson A, Windahl SH, Farman HH, et al. Probiotics protect mice from ovariectomy-induced cortical bone loss. PLoS One. 2014 1;9(3):e92368. [PubMed: 24637895]

27. Collins FL, Irwin R, Bierhalter H, Schepper J, Britton RA, Parameswaran N, et al. Lactobacillus reuteri 6475 Increases Bone Density in Intact Females Only under an Inflammatory Setting van Wijnen A, editor. PLoS One [Internet]. Public Library of Science; 2016 4 8 [cited 2016 Aug 30];11(4):e0153180. Available from: http://dx.plos.org/10.1371/journal.pone.0153180

28. Zhang J, Motyl KJ, Irwin R, MacDougald O a., Britton RA, McCabe LR Loss of Bone and Wnt10b Expression in Male Type 1 Diabetic Mice Is Blocked by the Probiotic Lactobacillus reuteri Endocrinology [Internet] Endocrine Society Chevy Chase, MD; 2015 9 2 [cited 2016 May 24];156(9):3169–82. Available from: http://www.ncbi.nlm.nih.gov/pubmed/26135835
29. Sjögren K, Engdahl C, Henning P, Lerner UH, Tremaroli V, Lagerquist MK, et al. The gut microbiota regulates bone mass in mice J Bone Miner Res [Internet]. Wiley Subscription Services, Inc., A Wiley Company; 2012 6 [cited 2015 Jul 5];27(6):1357–67. Available from: http://doi.wiley.com/10.1002/jbmr.1588
30. Quach D, Collins F, Parameswaran N, McCabe L, Britton RA. Microbiota Reconstitution Does Not Cause Bone Loss in Germ-Free Mice. mSphere [Internet]. American Society for Microbiology Journals; 2018 2 28 [cited 2018 Jan 22];3(1):e00545–17. Available from: http://www.ncbi.nlm.nih.gov/pubmed/29299532
31. Yan J, Herzog JW, Tsang K, Brennan CA, Bower MA, Garrett WS, et al. Gut microbiota induce IGF-1 and promote bone formation and growth. Proc Natl Acad Sci U S A [Internet]. National Academy of Sciences; 2016 11 22 [cited 2017 May 2];113(47):E7554–63. Available from: http://www.ncbi.nlm.nih.gov/pubmed/27821775
32. Wu H-J, Ivanov II, Darce J, Hattori K, Shima T, Umesaki Y, et al. Gut-Residing Segmented Filamentous Bacteria Drive Autoimmune Arthritis via T Helper 17 Cells. Immunity [Internet]. Cell Press; 2010 6 25 [cited 2018 Nov 7];32(6):815–27. Available from: https://www.sciencedirect.com/science/article/pii/S1074761310002049
33. Ivanov II, Atarashi K, Manel N, Brodie EL, Shima T, Karaoz U, et al. Induction of Intestinal Th17 Cells by Segmented Filamentous Bacteria. Cell [Internet]. Cell Press; 2009 10 30 [cited 2018 Nov 7];139(3):485–98. Available from: https://www.sciencedirect.com/science/article/pii/S0092867409012483
34. Schwarzer M, Makki K, Storelli G, Machuca-Gayet I, Srutkova D, Hermanova P, et al. Lactobacillus plantarum strain maintains growth of infant mice during chronic undernutrition. Science (80-) [Internet]. 2016 [cited 2016 Nov 18];351(6275). Available from: http://science.sciencemag.org/content/351/6275/854
35. Novince CM, Whittow CR, Aartun JD, Hathaway JD, Poulides N, Chavez MB, et al. Commensal Gut Microbiota Immunomodulatory Actions in Bone Marrow and Liver have Catabolic Effects on Skeletal Homeostasis in Health. Sci Rep [Internet]. Nature Publishing Group; 2017 12 18 [cited 2018 Oct 22];7(1):5747 Available from: http://www.nature.com/articles/s41598-017-06126-x
36. Guida F, Turco F, Iannotta M, De Gregorio D, Palumbo I, Sarnelli G, et al. Antibiotic-induced microbiota perturbation causes gut endocannabinoidome changes, hippocampal neuroglial reorganization and depression in mice. Brain Behav Immun [Internet]. 2018 1 [cited 2018 Jul 23];67:230–45. Available from: http://www.ncbi.nlm.nih.gov/pubmed/28890155
37. Miyoshi J, Bobe AM, Miyoshi S, Huang Y, Hubert N, Delmont TO, et al. Peripartum Antibiotics Promote Gut Dysbiosis, Loss of Immune Tolerance, and Inflammatory Bowel Disease in Genetically Prone Offspring. Cell Rep [Internet]. 2017 7 11 [cited 2018 Jul 23];20(2):491–504. Available from: http://www.ncbi.nlm.nih.gov/pubmed/28700948
38. Hooper LV, Littman DR, Macpherson AJ. Interactions between the microbiota and the immune system. Science [Internet]. NIH Public Access; 2012 6 8 [cited 2018 Jul 3];336(6086):1268–73. Available from: http://www.ncbi.nlm.nih.gov/pubmed/22674334
39. Schulfer AF, Battaglia T, Alvarez Y, Bijnens L, Ruiz VE, Ho M, et al. Intergenerational transfer of antibiotic-perturbed microbiota enhances colitis in susceptible mice. Nat Microbiol [Internet]. 2018 2 27 [cited 2018 Jul 30];3(2):234–42. Available from: http://www.ncbi.nlm.nih.gov/pubmed/29180726
40. Cho I, Yamanishi S, Cox L, Methe B a, Zavadil J, Li K, et al. Antibiotics in early life alter the murine colonic microbiome and adiposity. Nature [Internet]. Nature Publishing Group; 2012 8 22 [cited 2017 Jan 25];488(7413):621–6. Available from: http://www.nature.com/articles/nature11400
41. Holtom PD, Pavkovic SA, Bravos PD, Patzakis MJ, Shepherd LE, Frenkel B. Inhibitory effects of the quinolone antibiotics trovafloxacin, ciprofloxacin, and levofloxacin on osteoblastic cells in vitro. J Orthop Res [Internet]. 2000 9 [cited 2015 Apr 1];18(5):721–7. Available from: http://www.ncbi.nlm.nih.gov/pubmed/11117292

42. Scholz-Ahrens KE, Ade P, Marten B, Weber P, Timm W, Afil Y, et al. Prebiotics, probiotics, and synbiotics affect mineral absorption, bone mineral content, and bone structure. J Nutr [Internet]. 2007;137(3 Suppl 2):838S–46S. Available from: http://search.proquest.com/docview/197448991/fulltext/8618407F2DBC4B67PQ/1?accountid=12598
43. Guss JD, Horsfield MW, Fontenele FF, Sandoval TN, Luna M, Apoorva F, et al. Alterations to the Gut Microbiome Impair Bone Strength and Tissue Material Properties. J Bone Miner Res [Internet]. 2017 [cited 2017 Jun 7];32(6):1343–53. Available from: http://www.ncbi.nlm.nih.gov/pubmed/28244143
44. Jakobsson HE, Jernberg C, Andersson AFA, Sjölund-Karlsson M, Jansson JJK, Engstrand L, et al. Short-Term Antibiotic Treatment Has Differing Long-Term Impacts on the Human Throat and Gut Microbiome Ratner AJ, editor. PLoS One [Internet]. Public Library of Science; 2010 3 24 [cited 2016 Nov 14];5(3):e9836 Available from: http://dx.plos.org/10.1371/journal.pone.0009836
45. Jernberg C, Löfmark S, Edlund C, Jansson JK. Long-term ecological impacts of antibiotic administration on the human intestinal microbiota. ISME J [Internet]. 2007 5 1 [cited 2018 Jan 24];1(1):56–66. Available from: http://www.ncbi.nlm.nih.gov/pubmed/18043614
46. Ferrier L, Berard F, Debrauwer L, Chabo C, Langella P, Bueno L, et al. Impairment of the intestinal barrier by ethanol involves enteric microflora and mast cell activation in rodents. Am J Pathol [Internet]. American Society for Investigative Pathology; 2006 4 [cited 2017 Sep 5];168(4):1148–54. Available from: http://www.ncbi.nlm.nih.gov/pubmed/16565490
47. KIMURA T, ENDO H, YOSHIKAWA M, MURANISHI S, SEZAKI H Carriermediated transport systems for aminopenicillins in rat small intestine. J Pharmacobiodyn [Internet]. The Pharmaceutical Society of Japan; 1978 [cited 2017 Oct 26];1(4):262–7. Available from: http://joi.jlc.jst.go.jp/JST.Journalarchive/bpb1978/1.262?from=CrossRef
48. Tsuji A, Nakashima E, Kagami I, Yamana T. Intestinal Absorption Mechanism of Amphoteric P-Lactam Antibiotics I: Comparative Absorption and Evidence for In Situ Rat Small Intestine. [cited 2017 Oct 26]; Available from: http://onlinelibrary.wiley.com/store/10.1002/jps.2600700714/asset/2600700714_ftp.pdf?v=1&t=j98sjzl3&s=dbd5da6e6d1049ecc9265683f2c364d903cec6a8
49. Van Der Waaij D, Berghuis-De Vries JM, Altes CK. Oral dose and faecal concentration of antibiotics during antibiotic decontamination in mice and in a patient. J Hyg, Camb [Internet]. 1974 [cited 2017 Oct 26];73 Available from: https://www.ncbi.nlm.nih.gov/pmc/articles/PMC2130317/pdf/jhyg00074-0034.pdf
50. Bianchi ML. Inflammatory bowel diseases, celiac disease, and bone. Arch Biochem Biophys [Internet]. 2010 11 1 [cited 2017 Feb 15];503(1):54–65. Available from: http://www.ncbi.nlm.nih.gov/pubmed/20599670
51. Arrieta MC, Bistritz L, Meddings JB. Alterations in intestinal permeability. Gut [Internet]. BMJ Group; 2006 10 [cited 2017 Feb 20];55(10):1512–20. Available from: http://www.ncbi.nlm.nih.gov/pubmed/16966705
52. Rehman A, Sina C, Gavrilova O, Hasler R, Ott S, Baines JF, et al. Nod2 is essential for temporal development of intestinal microbial communities. Gut [Internet]. 2011 10 1 [cited 2017 Sep 14];60(10):1354–62. Available from: http://www.ncbi.nlm.nih.gov/pubmed/21421666
53. Porter A, Irwin R, Miller J, Horan DJ, Robling AG, McCabe LR. Quick and inexpensive paraffin-embedding method for dynamic bone formation analyses. Sci Rep [Internet]. Nature Publishing Group; 2017 2 15 [cited 2017 Jun 13];7:42505 Available from: http://www.nature.com/articles/srep42505
54. Dempster DW, Compston JE, Drezner MK, Glorieux FH, Kanis JA, Malluche H, et al. Standardized nomenclature, symbols, and units for bone histomorphometry: A 2012 update of the report of the ASBMR Histomorphometry Nomenclature Committee. J Bone Miner Res [Internet]. Wiley-Blackwell; 2013 1 1 [cited 2018 Oct 11];28(1):2–17. Available from: http://doi.wiley.com/10.1002/jbmr.1805
55. Gardinier JD, Rostami N, Juliano L, Zhang C. Bone adaptation in response to treadmill exercise in young and adult mice. Bone reports [Internet]. Elsevier; 2018 6 [cited 2018 Jul 26];8:29–37. Available from: http://www.ncbi.nlm.nih.gov/pubmed/29379848
56. Turner CH, Burr DB. Basic biomechanical measurements of bone: A tutorial. Bone [Internet]. Elsevier; 1993 7 1 [cited 2018 Jul 26];14(4):595–608. Available from: https://www.sciencedirect.com/science/article/pii/875632829390081K

57. Collins J, Auchtung JM, Schaefer L, Eaton KA, Britton RA. Humanized microbiota mice as a model of recurrent Clostridium difficile disease. Microbiome [Internet]. BioMed Central; 2015 8 20 [cited 2018 Jul 30];3:35 Available from: http://www.ncbi.nlm.nih.gov/pubmed/26289776

58. Kozich JJ, Westcott SL, Baxter NT, Highlander SK, Schloss PD. Development of a dual-index sequencing strategy and curation pipeline for analyzing amplicon sequence data on the MiSeq Illumina sequencing platform. Appl Environ Microbiol [Internet]. American Society for Microbiology; 2013 9 1 [cited 2018 Jul 30];79(17):5112–20. Available from: http://www.ncbi.nlm.nih.gov/pubmed/23793624

59. Team RC. R: a language and environment for statistical computing. [Internet]. R Foundation for Statistical Computing, Vienna, Austria 2017 Available from: https://www.r.project.org

60. McMurdie PJ, Holmes S. phyloseq: An R Package for Reproducible Interactive Analysis and Graphics of Microbiome Census Data Watson M, editor. PLoS One [Internet]. Public Library of Science; 2013 4 22 [cited 2018 Jul 30];8(4):e61217 Available from: http://dx.plos.org/10.1371/journal.pone.0061217

61. Tulstrup MV-L, Christensen EG, Carvalho V, Linninge C, Ahrne S, H0jberg O, et al. Antibiotic Treatment Affects Intestinal Permeability and Gut Microbial Composition in Wistar Rats Dependent on Antibiotic Class Loh G, editor. PLoS One [Internet]. Public Library of Science; 2015 12 21 [cited 2017 Jun 2];10(12):e0144854. Available from: http://dx.plos.org/10.1371/journal.pone.0144854

62. Shi Y, Zhao X, Zhao J, Zhang H, Zhai Q, Narbad A, et al. A mixture of Lactobacillus species isolated from traditional fermented foods promote recovery from antibiotic-induced intestinal disruption in mice. J Appl Microbiol [Internet]. Wiley/Blackwell (10.1111); 2018 3 [cited 2018 Jun 5];124(3):842–54. Available from: http://doi.wiley.com/10.1111/jam.13687

63. Valuckaite V, Zaborina O, Long J, Hauer-Jensen M, Wang J, Holbrook C, et al. Oral PEG 15–20 protects the intestine against radiation: role of lipid rafts. Am J Physiol Gastrointest Liver Physiol [Internet]. American Physiological Society; 2009 12 [cited 2018 Jan 22];297(6):G1041–52. Available from: http://www.ncbi.nlm.nih.gov/pubmed/19833862

64. Tlaskalová-Hogenová H, Stepánková R, Kozakova H, Hudcovic T, Vannucci L, Tucková L, et al. The role of gut microbiota (commensal bacteria) and the mucosal barrier in the pathogenesis of inflammatory and autoimmune diseases and cancer: contribution of germ-free and gnotobiotic animal models of human diseases. Cell Mol Immunol [Internet]. Nature Publishing Group; 2011 3 [cited 2018 Jul 19];8(2):110–20. Available from: http://www.ncbi.nlm.nih.gov/pubmed/21278760

65. Sun J, Shen X, Li Y, Guo Z, Zhu W, Zuo L, et al. Therapeutic Potential to Modify the Mucus Barrier in Inflammatory Bowel Disease. Nutrients [Internet]. Multidisciplinary Digital Publishing Institute (MDPI); 2016 1 14 [cited 2017 Apr 19];8(1). Available from: http://www.ncbi.nlm.nih.gov/pubmed/26784223

66. Vindigni SM, Zisman TL, Suskind DL, Damman CJ. The intestinal microbiome, barrier function, and immune system in inflammatory bowel disease: a tripartite pathophysiological circuit with implications for new therapeutic directions Therap Adv Gastroenterol [Internet]. SAGE Publications; 2016 7 [cited 2017 Mar 20];9(4):606–25. Available from: http://www.ncbi.nlm.nih.gov/pubmed/27366227

67. Ohlsson C, Sjögren K. Effects of the gut microbiota on bone mass. Trends Endocrinol Metab [Internet]. 2015 2 [cited 2015 Jun 18];26(2):69–74. Available from: http://www.sciencedirect.com/science/article/pii/S104327601400201X

68. McCabe LR, Irwin R, Tekalur A, Evans C, Schepper JD, Parameswaran N, et al. Exercise prevents high fat diet-induced bone loss, marrow adiposity and dysbiosis in male mice. Bone [Internet]. Elsevier; 2018 3 29 [cited 2018 Apr 9]; Available from: https://www.sciencedirect.com/science/article/pii/S8756328218301431#ab0010

69. Paul Cotter D., Caitriona Guinane M. Role of the gut microbiota in health and chronic gastrointestinal disease understanding a hidden metabolic organ. Ther Adv Gastroenterol [Internet]. 2013 [cited 2016 Aug 30];6(4):295–308. Available from: http://www.sagepub.co.uk/

70. Francino MP. Antibiotics and the Human Gut Microbiome: Dysbioses and Accumulation of Resistances Front Microbiol [Internet]. Frontiers Media SA; 2015 [cited 2017 Feb 9];6:1543 Available from: http://www.ncbi.nlm.nih.gov/pubmed/26793178

71. Langdon A, Crook N, Dantas G. The effects of antibiotics on the microbiome throughout development and alternative approaches for therapeutic modulation. Genome Med [Internet]. BioMed Central; 2016 4 13 [cited 2017 Apr 19];8(1):39 Available from: http://www.ncbi.nlm.nih.gov/pubmed/27074706
72. Mikkelsen KH, Frost M, Bahl MI, Licht TR, Jensen US, Rosenberg J, et al. Effect of Antibiotics on Gut Microbiota, Gut Hormones and Glucose Metabolism Buchowski M, editor. PLoS One [Internet]. Public Library of Science; 2015 11 12 [cited 2016 Aug 16];10(11):e0142352. Available from: http://dx.plos.org/10.1371/journal.pone.0142352
73. Bäumler AJ, Sperandio V. Interactions between the microbiota and pathogenic bacteria in the gut. Nature [Internet]. 2016 7 7 [cited 2018 Jul 23];535(7610):85–93. Available from: http://www.ncbi.nlm.nih.gov/pubmed/27383983
74. Becattini S, Taur Y, Pamer EG. Antibiotic-Induced Changes in the Intestinal Microbiota and Disease. Trends Mol Med [Internet]. NIH Public Access; 2016 [cited 2018 Jul 23];22(6):458–78. Available from: http://www.ncbi.nlm.nih.gov/pubmed/27178527
75. Chung H, Pamp SJ, Hill JA, Surana NK, Edelman SM, Troy EB, et al. Gut Immune Maturation Depends on Colonization with a Host-Specific Microbiota. Cell [Internet]. 2012 6 22 [cited 2017 Sep 12];149(7):1578–93. Available from: http://www.ncbi.nlm.nih.gov/pubmed/22726443
76. Leser TD, M0lbak L Better living through microbial action: the benefits of the mammalian gastrointestinal microbiota on the host. Environ Microbiol [Internet]. 2009 9 [cited 2017 Jun 27];11(9):2194–206. Available from: http://www.ncbi.nlm.nih.gov/pubmed/19737302
77. Weinstein RS, Jilka RL, Parfitt AM, Manolagas SC. Inhibition of Osteoblastogenesis and Osteocytes by Glucocorticoids Potential Mechanisms of Their Deleterious Effects on Bone. J Clin Invest [Internet]. 1998 [cited 2017 Mar 28];102(2):274–82. Available from: http://www.jci.org
78. Collins SM. A role for the gut microbiota in IBS. Nat Rev Gastroenterol Hepatol [Internet]. 2014 8 22 [cited 2018 Jul 10];11(8):497–505. Available from: http://www.ncbi.nlm.nih.gov/pubmed/24751910
79. Larsen N, Vogensen FK, van den Berg FWJ, Nielsen DS, Andreasen AS, Pedersen BK, et al. Gut microbiota in human adults with type 2 diabetes differs from non-diabetic adults. PLoS One [Internet]. 2010 1 5 [cited 2014 Jul 10];5(2):e9085 Available from: http://journals.plos.org/plosone/article?id=10.1371/journal.pone.0009085#s2
80. Carmody RN, Gerber GK, Luevano JM, Gatti DM, Somes L, Svenson KL, et al. Diet dominates host genotype in shaping the murine gut microbiota. Cell Host Microbe [Internet]. Cell Press; 2015 1 14 [cited 2017 Sep 13];17(1):72–84. Available from: http://www.sciencedirect.com/science/article/pii/S1931312814004260
81. Irwin R, Raehtz S, Parameswaran N, McCabe LR. Intestinal inflammation without weight loss decreases bone density and growth. Am J Physiol-Regul Integr Comp Physiol [Internet]. 2016 [cited 2017 Jun 22];311(6). Available from:http://ajpregu.physiology.org.proxy1.cl.msu.edU/content/311/6/R1149
82. Raehtz S, Hargis BM, Kuttappan VA, Pamukcu R, Bielke LR, McCabe LR. High Molecular Weight Polymer Promotes Bone Health and Prevents Bone Loss Under Salmonella Challenge in Broiler Chickens Front Physiol [Internet]. Frontiers; 2018 4 13 [cited 2018 Jul 23];9:384 Available from: http://journal.frontiersin.org/article/10.3389/fphys.2018.00384/full.
83. Bernstein CN, Leslie WD. The pathophysiology of bone disease in gastrointestinal disease. Eur J Gastroenterol Hepatol [Internet]. 2003 8 [cited 2016 Sep 22];15(8):857–64. Available from: http://www.ncbi.nlm.nih.gov/pubmed/12867794
84. Dresner-Pollak R, Gelb N, Rachmilewitz D, Karmeli F, Weinreb M. Interleukin 10-deficient mice develop osteopenia, decreased bone formation, and mechanical fragility of long bones. Gastroenterology [Internet]. Elsevier; 2004 9 1 [cited 2018 Oct 22];127(3):792–801. Available from: http://linkinghub.elsevier.com/retrieve/pii/S0016508504010340
85. Bron PA, Kleerebezem M, Brummer R-J, Cani PD, Mercenier A, MacDonald TT, et al. Can probiotics modulate human disease by impacting intestinal barrier function? Br J Nutr [Internet]. Cambridge University Press; 2017 1 [cited 2017 Jun 27];117(1):93–107. Available from: http://www.ncbi.nlm.nih.gov/pubmed/28102115
86. Anderson RC, Cookson AL, McNabb WC, Kelly WJ, Roy NC. Lactobacillus plantarum DSM 2648 is a potential probiotic that enhances intestinal barrier function. FEMS Microbiol Lett

[Internet]. 2010 7 2 [cited 2017 May 3];309(2):no-no. Available from: http://www.ncbi.nlm.nih.gov/pubmed/20618863

87. Mennigen R, Nolte K, Rijcken E, Utech M, Loeffler B, Senninger N, et al. Probiotic mixture VSL#3 protects the epithelial barrier by maintaining tight junction protein expression and preventing apoptosis in a murine model of colitis. Am J Physiol - Gastrointest Liver Physiol. 2009;296(5).
88. Mariman R, Kremer B, Koning F, Nagelkerken L. The probiotic mixture VSL#3 mediates both pro- and anti-inflammatory responses in bone marrow-derived dendritic cells from C57BL/6 and BALB/c mice. Br J Nutr [Internet]. 2014 10 2 [cited 2017 May 3];112(07):1088–97. Available from: http://www.ncbi.nlm.nih.gov/pubmed/25181025
89. Gatej SM, Marino V, Bright R, Fitzsimmons TR, Gully N, Zilm P, et al. Probiotic Lactobacillus rhamnosus GG prevents alveolar bone loss in a mouse model of experimental periodontitis. J Clin Periodontol [Internet]. 2018 2 [cited 2018 Oct 11];45(2):204–12. Available from: http://www.ncbi.nlm.nih.gov/pubmed/29121411
90. Szajewska H, Kolodziej M. Systematic review with meta-analysis: Lactobacillus rhamnosus GG in the prevention of antibiotic-associated diarrhoea in children and adults. Aliment Pharmacol Ther [Internet]. 2015 11 [cited 2017 May 2];42(10):1149–57. Available from: http://www.ncbi.nlm.nih.gov/pubmed/26365389
91. Bousvaros A, Guandalini S, Baldassano RN, Botelho C, Evans J, Ferry GD, et al. A Randomized, Double-blind Trial of Lactobacillus GG Versus Placebo in Addition to Standard Maintenance Therapy for Children with Crohn's Disease. [cited 2017 Jun 26]; Available from: https://insights.ovid.com/pubmed?pmid=16116318
92. Ardita CS, Mercante JW, Kwon YM, Luo L, Crawford ME, Powell DN, et al. Epithelial Adhesion Mediated by Pilin SpaC Is Required for Lactobacillus rhamnosus GG-Induced Cellular Responses. Appl Environ Microbiol [Internet]. 2014 8 15 [cited 2017 Sep 12];80(16):5068–77. Available from: http://aem.asm.org/cgi/doi/10.1128/AEM.01039-14
93. Thomas CM, Hong T, van Pijkeren JP, Hemarajata P, Trinh DV, Hu W, et al. Histamine derived from probiotic Lactobacillus reuteri suppresses TNF via modulation of PKA and ERK signaling. PLoS One [Internet]. Public Library of Science; 2012 [cited 2017 Sep 12];7(2):e31951 Available from: http://www.ncbi.nlm.nih.gov/pubmed/22384111
94. Lin YP, Thibodeaux CH, Peña JA, Ferry GD, Versalovic J. Probiotic Lactobacillus reuteri Suppress Proinflammatory Cytokines via c - Jun Background : Differential immunoregulatory capabilities of pro.
95. Motyl KJ, McCauley LK, McCabe LR. Amelioration of type I diabetes-induced osteoporosis by parathyroid hormone is associated with improved osteoblast survival J Cell Physiol [Internet]. Wiley-Blackwell; 2012 4 [cited 2018 Jul 23];227(4):1326–34. Available from: http://doi.wiley.com/10.1002/jcp.22844
96. Harris L, Senagore P, Young VB, McCabe LR. Inflammatory bowel disease causes reversible suppression of osteoblast and chondrocyte function in mice. Am J Physiol - Gastrointest Liver Physiol [Internet]. 2009 [cited 2017 May 3];296(5). Available from: http://ajpgi.physiology.org/content/296/5/g1020.full
97. Berek L, Banos S. Studies on young Germ-Free Mice. Acta Microbiol Acad Sci Hung [Internet]. 1971;18(4):283–9. Available from: file:///Users/jonathanschepper/Downloads/AGlt1E-986084.pdf
98. Winter S, Ratner A, Nelson A, Weiser J, Benoist C, Mathis D. Deciphering the tête-à-tête between the microbiota and the immune system Nature [Internet]. American Society for Clinical Investigation; 2014 10 1 [cited 2017 Sep 12];467(7314):426–9. Available from: https://www.jci.org/articles/view/72332
99. Macpherson AJ, Gatto D, Sainsbury E, Harriman GR, Hengartner H, Zinkernagel RM. A primitive T cell-independent mechanism of intestinal mucosal IgA responses to commensal bacteria. Science [Internet]. 2000 6 23 [cited 2018 Jul 3];288(5474):2222–6. Available from: http://www.ncbi.nlm.nih.gov/pubmed/10864873
100. Cox LM, Yamanishi S, Sohn J, Alekseyenko AV, Leung JM, Cho I, et al. Altering the intestinal microbiota during a critical developmental window has lasting metabolic consequences. Cell [Internet]. NIH Public Access; 2014 8 14 [cited 2016 Sep 9];158(4):705–21. Available from: http://www.ncbi.nlm.nih.gov/pubmed/25126780

101. Erkosar B, Storelli G, Defaye A, Leulier F. Host-Intestinal Microbiota Mutualism: "Learning on the Fly." Cell Host Microbe [Internet]. 2013 1 16 [cited 2017 Nov 21];13(1):8–14. Available from: http://www.ncbi.nlm.nih.gov/pubmed/23332152

102. Hyun S Body size regulation and insulin-like growth factor signaling Cell Mol Life Sci [Internet]. SP Birkhäuser Verlag Basel; 2013 7 19 [cited 2017 Jun 26];70(13):2351–65. Available from: http://link.springer.com/10.1007/s00018-013-1313-5

103. Suez J, Zmora N, Zilberman-Schapira G, Mor U, Dori-Bachash M, Bashiardes S, et al. Post-Antibiotic Gut Mucosal Microbiome Reconstitution Is Impaired by Probiotics and Improved by Autologous FMT. Cell [Internet]. Cell Press; 2018 9 6 [cited 2018 Sep 26];174(6):1406–1423.e16. Available from: https://www.sciencedirect.com/science/article/pii/S0092867418311085?via%3Dihub

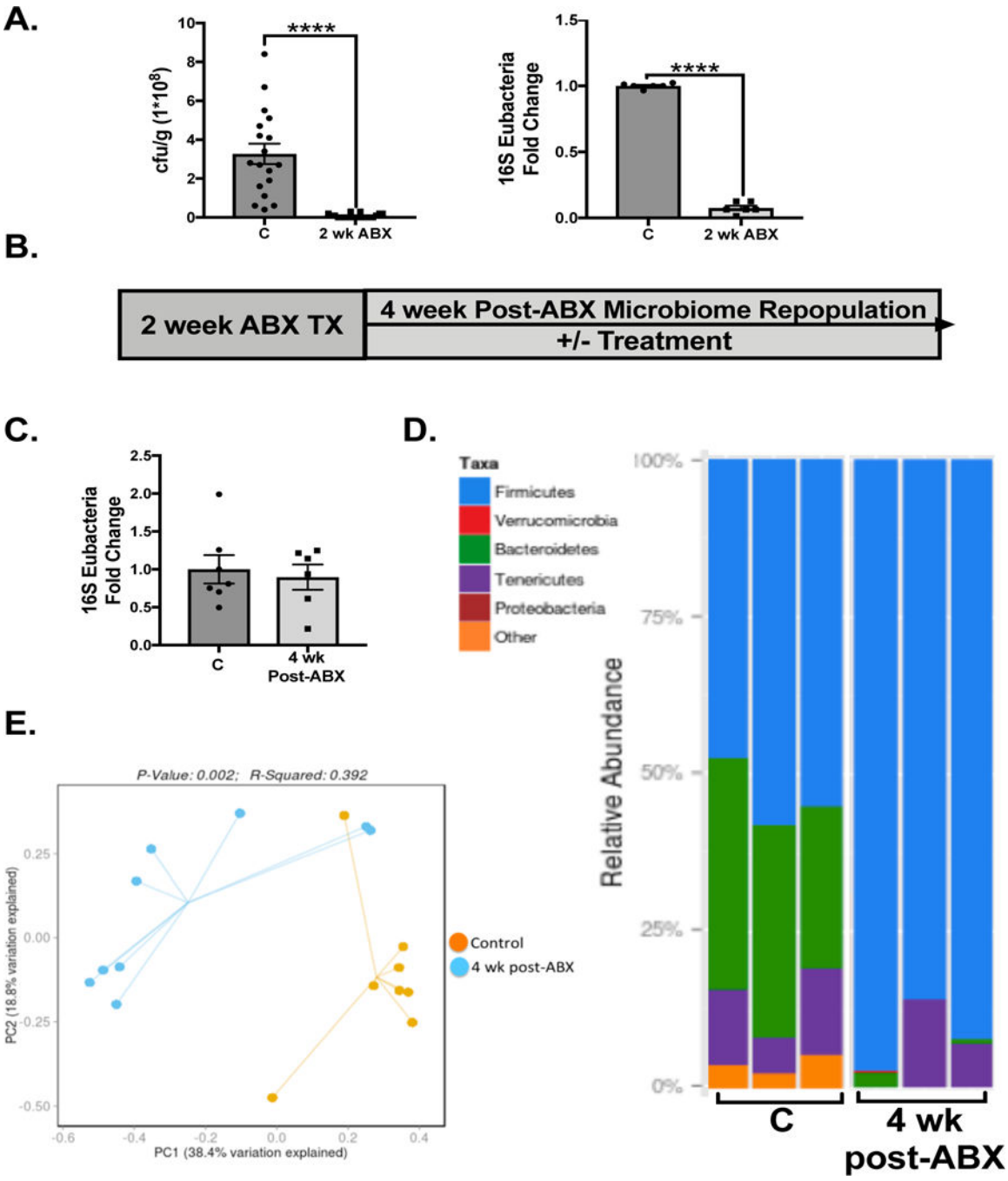

Figure 1: Impact of 2-week ABX treatment on the intestinal microbiota immediately and 4-weeks post-ABX treatment.

12-week-old male BALB/c mice were given sterile water or ABX (ampicillin and neomycin) for 2-weeks to deplete the intestinal microbiota. A) Fecal samples, from control and 2-week ABX treated mice, were plated on agar dishes to determine number of colony forming units (cfu)(n=18–20). Additionally, bacterial 16S rRNA was analyzed to assess levels of total eubacteria (n=6). B) The experimental design used to induce post-ABX dysbiosis. C) Total eubacteria levels were assed from control and 4-week post-ABX treated mice in first experimental run (n=6–7). D) Relative abundance of bacterial taxa in control and 4-week

post-ABX fecal samples (n=3). Statistical analysis performed by Student's t-test E) PCoA plot of fecal microbiome data, Bray-Curtis analysis performed to determine significance (n=8–9). Values are average ± SEM. **** $p<0.0001$.

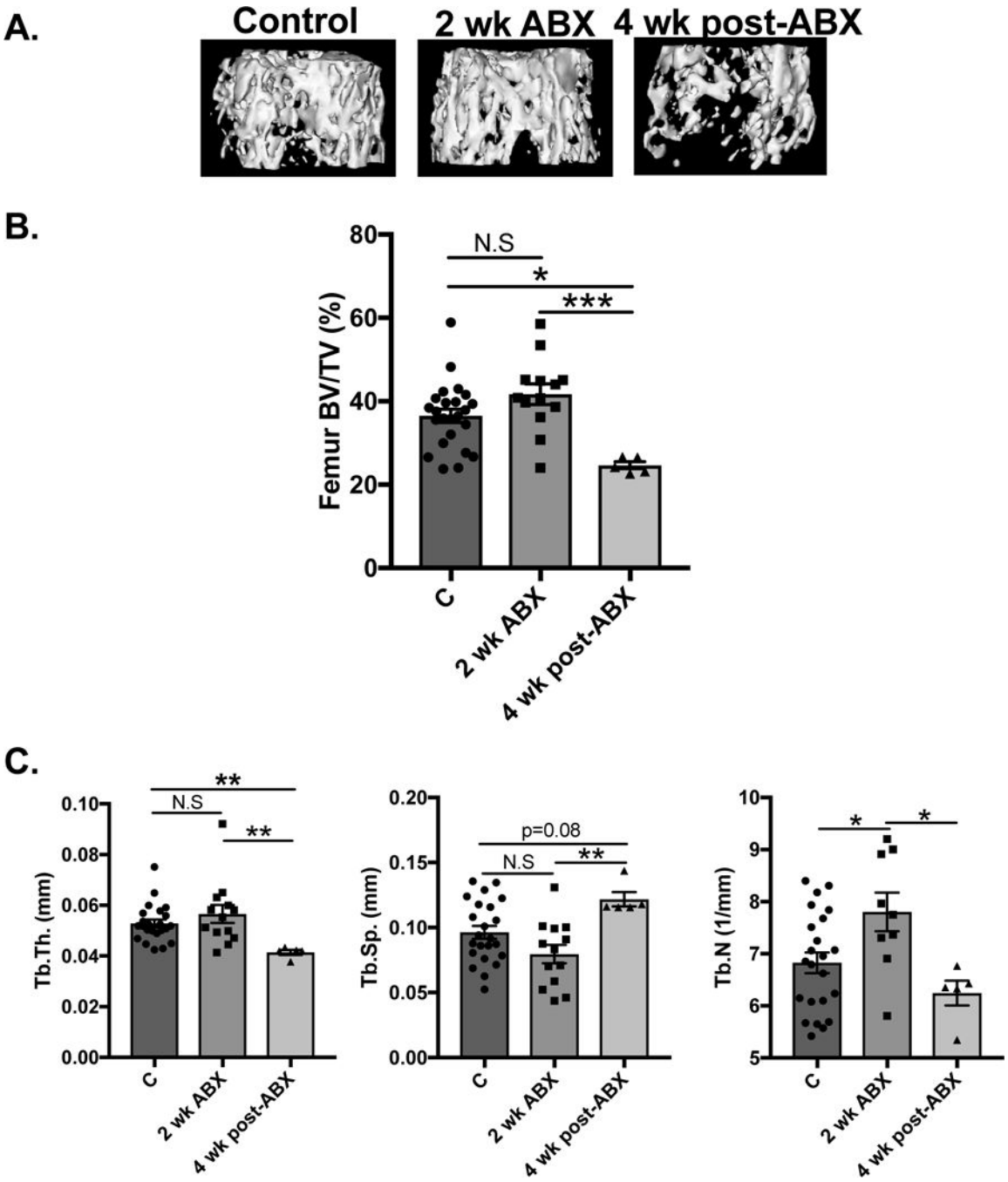

Figure 2: Effect of 2-week ABX treatment and subsequent 4-week natural microbiota repopulation on distal femur trabecular bone volume and architecture.

12-week-old male BALB/c mice were given sterile water or antibiotics for 2-weeks followed by sterile water for 4-weeks. A-B) Distal femoral metaphyseal trabecular bone volume was investigated at 2 weeks of antibiotic treatment and 4-weeks post- ABX treatment (n= 24,13,5 respectably). C) Femoral bone architecture measures in control versus 2- weeks ABX and 4-weeks post-ABX mice (n= 24,13,5 respectably). Values are average ± SEM. Statistical analysis performed with 1-way ANOVA with Tukey post-test. *** $p<0.001$;** $p<0.01$; *$p<0.05$.

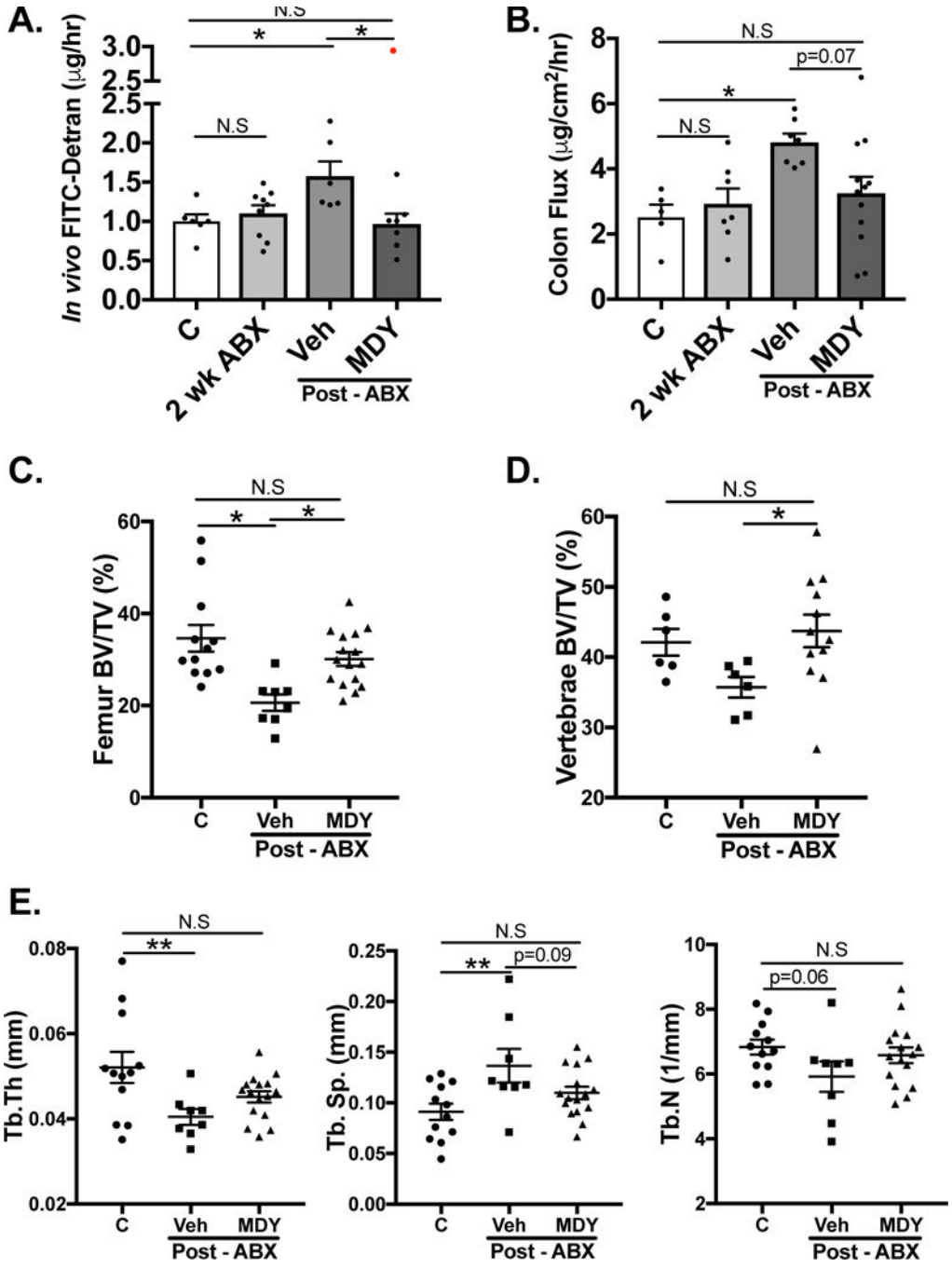

Figure 3: MDY supplementation prevents increased intestinal permeability and bone loss.

12-week-old male BALB/c mice were untreated (controls) or treated with ABX for 2 weeks. Post-ABX mice were given sterile water (Veh) or supplemented a high molecular weight polymer (MDY). A) Whole intestinal in vivo flux was measured by FITC dextran gavage (n=6–8). B) Colon sections were analyzed ex vivo. 4-kDa FITC flux was measured in ussing chambers (n=5–12). C-D) MicroCT analysis of femoral and vertebral trabecular bone volume fraction (n=6–16). E) Femoral bone microarchitecture [J.CT analyses (n=8–16)

Values are average ± SEM. Statistical analysis was performed with 1-way ANOVA with Tukey post-test. ** $p<0.01$; *$p<0.05$. Outlier excluded from data analysis shown in red.

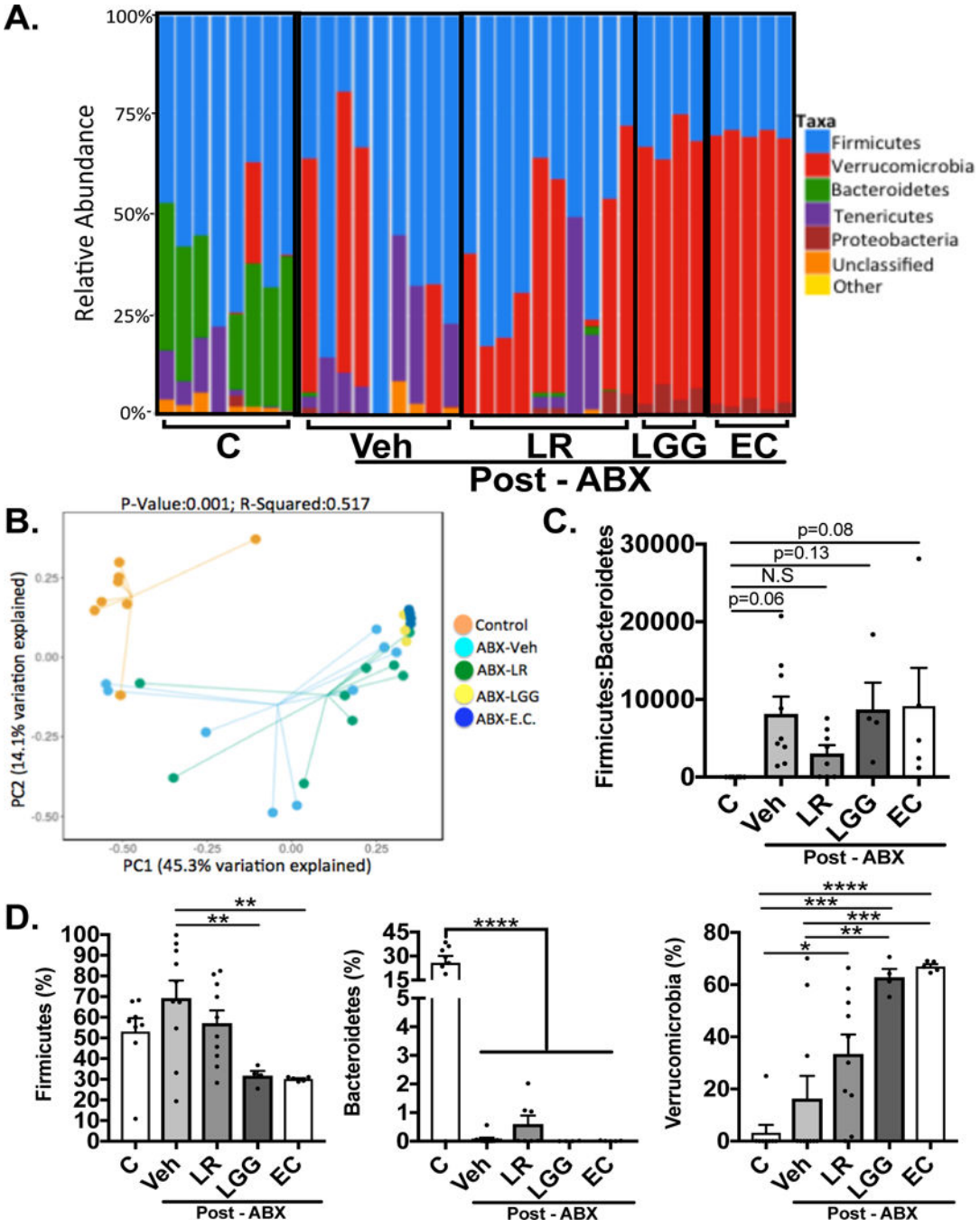

Figure 4: Gut microbiome supplementation following antibiotics affects intestinal microbial composition.

12-week-old BALB/c male mice were untreated (controls) or treated with ABX for 2 weeks. Post-ABX mice were either given sterile water (Veh) or supplemented with *L. reuteri* (LR), *Lactobacillus rhamnosus* GG (LGG) or non-pathogenic *Escherichia coli* (EC) for 4 weeks. A) Relative abundances of bacterial communities following gut supplementation. B) PCoA plot of fecal microbiome, Bray-Curtis analysis performed. Analysis of operational taxonomic units (OTUs) classified to the phylum's C) *Firmicutes* to *Bacteroidetes* ratio D) *Firmicutes, Bacteroidetes* and *Verrucomicrobia*. n = 8,9,10,4,5 respectively per group,

Values are average ± SEM. Statistical analysis of operational taxonomic units were performed by 1-way ANOVA with Tukey posttest. **** $p<0.0001$; *** $p<0.001$; ** $p<0.01$.

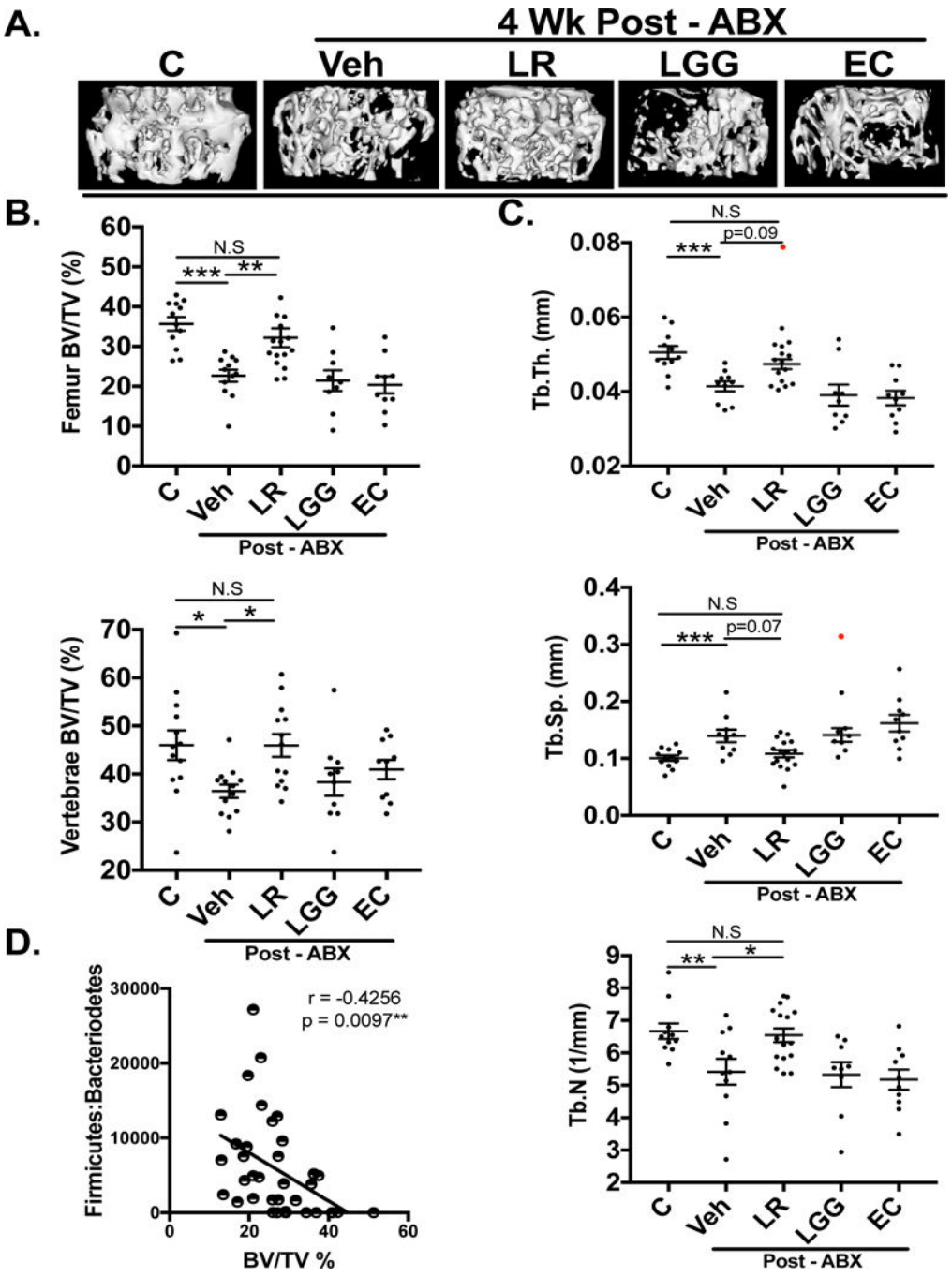

Figure 5: *L. reuteri* prevents bone loss following ABX treatment.

A) Representative |iCT isosurface images of control, antibiotic treated ± *L. reuteri*, LGG or EC. B) MicroCT analysis of femoral and vertebral trabecular bone volume fraction (n=9–16). C) Bone femur microarchitecture μCT analyses. (n=9–16) D) Correlation between bone volume fraction and *Firmicutes* to *Bacteroidetes* ratio. Both LGG and EC cohorts were statistically significant compared to controls in femoral BV/TV (%) and femur microarchitecture ($p<0.05$). Values are average ± SEM. Statistical analysis was performed

with 1-way ANOVA with Tukey post-test. *** $p<0.001$; ** $p<0.01$; *$p<0.05$. Outliers excluded from data analysis shown in red.

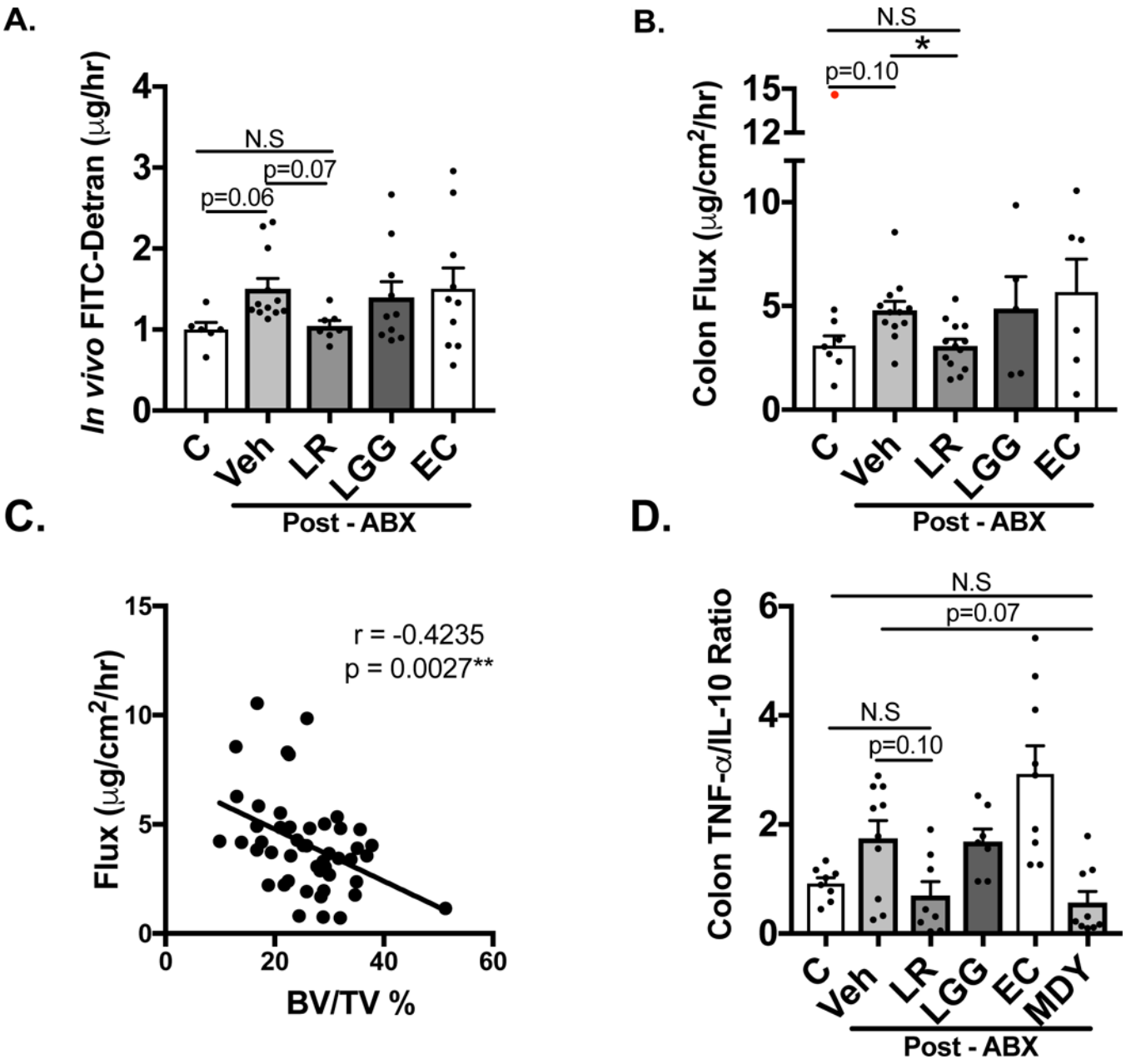

Figure 6: *L. reuteri* prevents increased gut permeability caused by antibiotic induced dysbiosis.

To examine how the post-ABX treatments altered intestinal permeability. A) Whole in vivo intestinal flux was measured by 4-kDa FITC dextran gavage (n=6–12). B) Colon sections were analyzed ex vivo. 4-kDa FITC flux was measured in ussing chambers (n=5–13. C) Correlation between Colon flux measures and femoral trabecular BV/TV % in all mice that underwent 4-week post ABX +/− treatments. Number of XY pairs observed is 49. D) Colon RNA gene expression of TNF-α /IL-10 ratio (n=8–10). Both LGG and EC cohorts were not statistically significant compared to controls. Values are average ± SEM. Statistical analysis was performed with 1-way ANOVA with Tukey post-test. ** p<0.01, *p<0.05. Outlier excluded from data analysis shown in red.

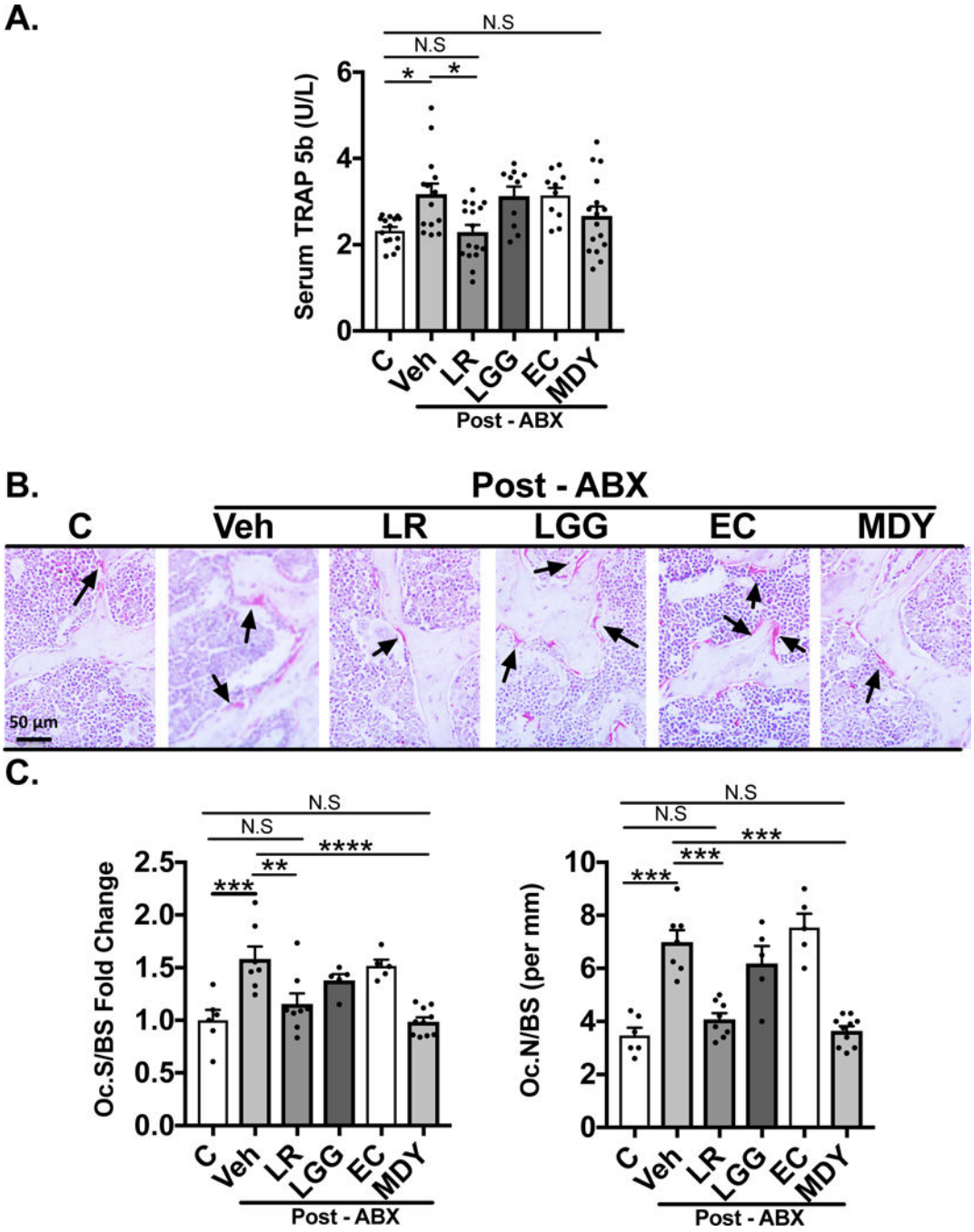

Figure 7. *L. reuteri* and MDY prevent increase in bone resorption markers induced by antibiotic microbial repopulation.

A) Serum TRAP 5b levels (n=10–15). B) Representative images of TRAP staining on section of the distal femoral trabecular region. C) Quantification of TRAP stain, osteoclast number and osteoclast surface/total bone surface in distal femur trabecular bone region (n=5–8). Both LGG and EC cohorts were statistically significant to controls in all resorption analyses ($p<0.05$). Values are average ± SEM. Statistical analysis was performed with 1-way ANOVA with Tukey post-test. **** $p<0.0001$; *** $p<0.001$; ** $p<0.01$; *$p<0.05$.

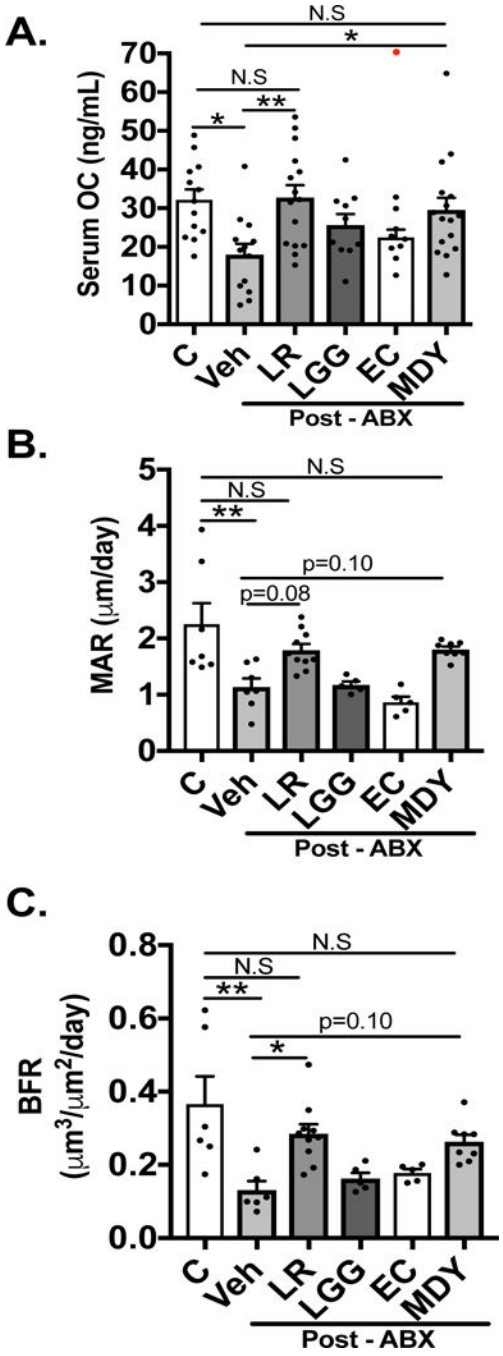

Figure 8: *L. reuteri* and MDY prevent imbalance of bone formation markers induced by antibiotic microbial repopulation.

A) Serum levels of bone formation marker osteocalcin (OC) (n=10–13). B) Quantitation of trabecular bone mineral apposition rate (MAR)(n=5–10). C) Quantitation of trabecular bone formation rate (BFR)(n=5–10). Both LGG and EC cohorts were statistically significantly compared to controls in MAR/BFR analysis ($p<0.05$). Values are average ± SEM. Statistical analysis was performed with 1-way ANOVA with Tukey post-test. *** $p<0.001$; ** $p<0.01$; *$p<0.05$. Outlier excluded from data analysis shown in red.

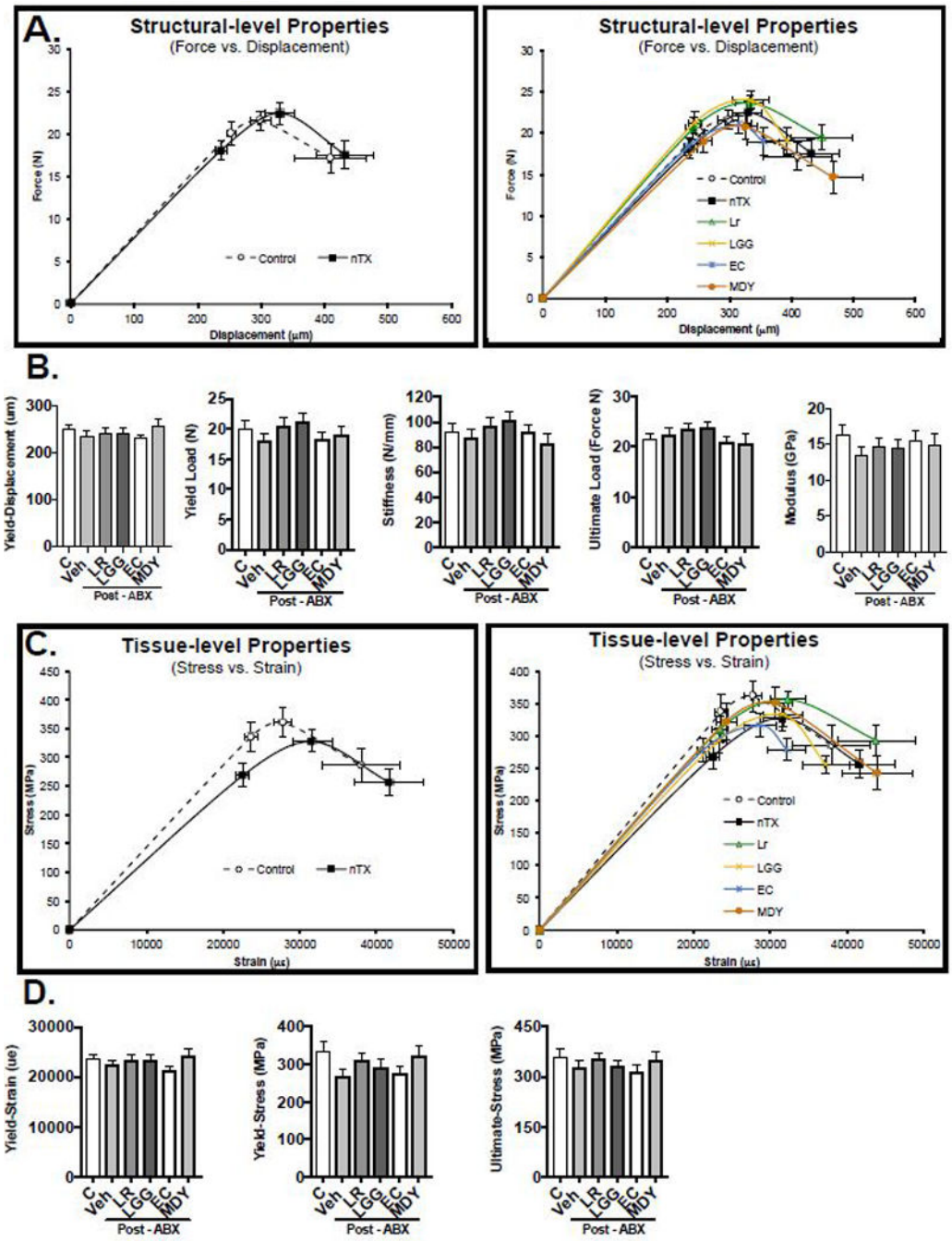

Figure 9: Microbial Manipulation does not Alter Mechanical Bone Properties.

Analysis of tibia (A and B) structural and (C and D) tissue level properties. Values are average ± SEM. n = 8–12 per group Statistical analysis was performed with 1 way ANOVA with Tukey post-test.

Table 1:
Antibiotic treatment does not change general body parameters.

Body weight, inguinal fat, retroperitoneal fat, kidney, spleen and liver were weighed after 2-weeks of ABX and 4-weeks of treatment. Values are averages ± SE. Statistical analysis was performed with 1-way ANOVA with Tukey post-test.

Body Weight Parameters (n)	Control (18)	ABX (18)	ABX+LR (16)	ABX+LGG (10)	ABX+E.C. (10)	ABX+MDY (16)
Body weight (g)	29.1 ± 0.5	28.4 ± 0.5	28.3 ± 0.4	29.05 ± 0.8	29.0 ± 0.5	28.6 ± 0.4
Liver (g)	1.5 ± 0.03	1.40 ± 0.05	1.43 ± 0.06	1.39 ± 0.05	1.39 ± 0.5	1.35 ± 0.06
Inguinal Fat (g)	0.11 ± 0.01	0.13 ± 0.02	0.15 ± 0.01	0.11 ± 0.02	0.11 ± 0.01	0.12 ± 0.01
Retroperitoneal Fat (mg)	49.7 ± 4.2	49.7 ± 5.4	56.3 ± 9.1	55.5 ± 9.0	58 ± 5.0	48.8 ± 8.9
Kidney (g)	0.25 ± 0.01	0.24 ± 0.01	0.25 ± 0.01	0.25 ± 0.01	0.25 ± 0.01	0.24 ± 0.01
Spleen (mg)	87.9 ± 2.1	91.1 ± 4.4	88.3 ± 3.0	91.4 ± 4.6	89.2 ± 3.3	92.8 ± 3.0

Table 2

Analyses of femoral cortical bone parameters.

Cortical area (Ct.Ar); cortical thickness (Ct.Th); marrow area (Ma.Ar); total area (Tt.Ar); bone mineral density (BMD); bone mineral content (BMC); inner perimeter and outer perimeter. Values are averages ± SE. n = 10–16 per group. Nothing significant compared to control. Statistical analysis was performed with 1-way ANOVA with Tukey post-test.

Cortical Parameters (n)	Control (18)	ABX (18)	ABX+LR (16)	ABX+LGG (10)	ABX+E.C. (10)	ABX+MDY (16)
Ct.Ar (mm^2)	1.08 ± 0.05	1.02 ± 0.03	1.03 ± 0.04	1.01 ± 0.02	1.05 ± 0.03	1.05 ± 0.02
Ct.Th (mm)	0.29 ± 0.01	0.28 ± 0.003	0.29 ± 0.003	0.29 ± 0.003	0.28 ± 0.005	0.28 ± 0.005
Ma.Ar (mm^2)	0.65 ± 0.04	0.62 ± 0.04	0.64 ± 0.03	0.61 ± 0.05	0.65 ± 0.02	0.60 ± 0.02
Tt.Ar (mm^2)	1.39 ± 0.10	1.42 ± 0.08	1.38 ± 0.09	1.5 ± 0.05	1.53 ± 0.05	1.4 ± 0.06
BMD (mg/cc)	1019 ± 24.34	1024 ± 18.5	1045 ± 39.05	1044 ± 55.7	1043 ± 27.23	1021 ± 27.02
BMC (mg)	0.022 ± 0.001	0.021 ± 0.0005	0.022 ± 0.001	0.022 ± 0.001	0.023 ± 0.0007	0.021 ± 0.001
Inner Perimeter (mm)	3.12 ± 0.09	3.03 ± 0.09	3.06 ± 0.08	3.05 ± 0.12	3.14 ± 0.05	3.00 ± 0.05
Outer Perimeter (mm)	4.91 ± 0.13	4.75 ± 0.11	4.8 ± 0.11	4.79 ± 0.14	4.75 ± 0.08	4.74 ± 0.05